MASTER'S THESIS

SURFACE MODIFICATION OF ORTHODONTIC BRACKET MODELS VIA ION IMPLANTATION: EFFECT ON COEFFICIENTS OF FRICTION

by

Stephen Walter Andrews, D.M.D.

The University of North Carolina
at Chapel Hill
Department of Orthodontics
School of Dentistry

1989

Robert P. Kusy
Advisor

Robert R. Reeber
Reader

Gary J. Dilley
Reader

SECURITY CLASSIFICATION OF THIS PAGE

REPORT DOCUMENTATION PAGE

Form Approved
OMB No. 0704-0188

1a. REPORT SECURITY CLASSIFICATION UNCLASSIFIED	1b. RESTRICTIVE MARKINGS NONE
2a. SECURITY CLASSIFICATION AUTHORITY	3. DISTRIBUTION / AVAILABILITY OF REPORT APPROVED FOR PUBLIC RELEASE; DISTRIBUTION UNLIMITED.
2b. DECLASSIFICATION / DOWNGRADING SCHEDULE	
4. PERFORMING ORGANIZATION REPORT NUMBER(S)	5. MONITORING ORGANIZATION REPORT NUMBER(S) AFIT/CI/CIA- 89-093
6a. NAME OF PERFORMING ORGANIZATION AFIT STUDENT AT UNIV OF NC 6b. OFFICE SYMBOL (If applicable)	7a. NAME OF MONITORING ORGANIZATION AFIT/CIA
6c. ADDRESS (City, State, and ZIP Code)	7b. ADDRESS (City, State, and ZIP Code) Wright-Patterson AFB OH 45433-6583
8a. NAME OF FUNDING / SPONSORING ORGANIZATION 8b. OFFICE SYMBOL (If applicable)	9. PROCUREMENT INSTRUMENT IDENTIFICATION NUMBER
8c. ADDRESS (City, State, and ZIP Code)	10. SOURCE OF FUNDING NUMBERS PROGRAM ELEMENT NO. / PROJECT NO. / TASK NO. / WORK UNIT ACCESSION NO.

11. TITLE (Include Security Classification) (UNCLASSIFIED)
SURFACE MODIFICATION OF ORTHODONTIC BRACKET MODELS VIA ION IMPLANTATION: EFFECT ON COEFRICIENTS OF FRICTION

12. PERSONAL AUTHOR(S)
STEPHEN WALTER ANDREWS

13a. TYPE OF REPORT	13b. TIME COVERED	14. DATE OF REPORT (Year, Month, Day)	15. PAGE COUNT
THESIS/~~DISSERTATION~~	FROM _____ TO _____	1989	75

16. SUPPLEMENTARY NOTATION
APPROVED FOR PUBLIC RELEASE IAW AFR 190-1
ERNEST A. HAYGOOD, 1st Lt, USAF
Executive Officer, Civilian Institution Programs

17. COSATI CODES			18. SUBJECT TERMS (Continue on reverse if necessary and identify by block number)
FIELD	GROUP	SUB-GROUP	

19. ABSTRACT (Continue on reverse if necessary and identify by block number)

20. DISTRIBUTION / AVAILABILITY OF ABSTRACT	21. ABSTRACT SECURITY CLASSIFICATION
☒ UNCLASSIFIED/UNLIMITED ☐ SAME AS RPT. ☐ DTIC USERS	UNCLASSIFIED

22a. NAME OF RESPONSIBLE INDIVIDUAL	22b. TELEPHONE (Include Area Code)	22c. OFFICE SYMBOL
ERNEST A. HAYGOOD, 1st Lt, USAF	(513) 255-2259	AFIT/CI

DD Form 1473, JUN 86 *Previous editions are obsolete.* SECURITY CLASSIFICATION OF THIS PAGE

AFIT/CI "OVERPRINT"

SURFACE MODIFICATION OF ORTHODONTIC BRACKET MODELS VIA ION IMPLANTATION: EFFECT ON COEFFICIENTS OF FRICTION

by

Stephen Walter Andrews, D.M.D.

A Thesis submitted to the faculty of
The University of North Carolina at
Chapel Hill in partial fulfillment of the
requirements for the degree of
Master of Science in the Department of
Orthodontics in the
School of Dentistry

Chapel Hill

1989

Approved by:

Robert P. Kusy
Advisor

Reader

Reader

ABSTRACT

STEPHEN W. ANDREWS. Surface Modification of Orthodontic Bracket Models via Ion Implantation: Effect on Coefficients of Friction. (under the direction of ROBERT P. KUSY, PH.D.)

In an effort to reduce the unwanted effects of friction, ion implantation of bracket models was accomplished and tested against the four major orthodontic alloy groups, [stainless steel (S.S.), cobalt-chromium (Co-Cr), nickel-titanium (NiTi), and beta-titanium (β-Ti)]. Stainless steel right-hand cylinders, 1/4" x 1/2", simulated orthodontic brackets. In addition to control samples, the polished faces of these cylinders were implanted with N+, Ti+/N+, N+/C+, N+/Cr+, Ti+, Ti+/C+, and C+. All were implanted at 2 x $10^{17}/cm^2$ except Ti+ (4 x $10^{17}/cm^2$) and Cr+ (3 x $10^{17}/cm^2$). Quality control was insured using Auger spectroscopy, specular reflectometry, and microhardness tests. Using an Instron tester the two cylinder flats were drawn along each arch wire at 1cm/min at 34°C in saliva. Frictional forces were measured, and both the coefficient of static friction, μ_s, and the coefficient of kinetic (sliding) friction, μ_k, were determined while varying the normal forces from 0.2 to 1kg.

The kinetic coefficients of the arch wires against the control S.S. models measured 0.163, 0.143, 0.240, and 0.312, respectively ($P \leq 0.01$). Results reveal that, with few exceptions, the S.S. control cylinders yielded lower μ_k's than the implanted cylinders. Any improvement seen with the implantations were marginal at best.

ACKNOWLEDGEMENTS

To my wife, Deborah, and my children, Marie and Shannon, for their support, patience, and love during this experience.

To Dr. Robert P. Kusy for his wisdom and guidance throughout this project.

To Drs. Robert R. Reeber and Gary J. Dilley for their productive recommendations.

To John Q. Whitley for his generous technical assistance.

To Dr. William R. Proffit for the opportunity to study orthodontics and to develop concepts I will use the rest of my life.

To the following persons and facilities for their technical expertise and gratis ion implantations:

Drs. Ward Halverson and Piran Sioshansi, Spire Corporation

Dr. Jim Williams, Oak Ridge National Laboratory

Dr. Jim Wortman, North Carolina State University

To Unitek Corporation, Rocky Mountain Orthodontics, and Ormco Corporation for their contribution of arch wires.

TABLE OF CONTENTS

LIST OF TABLES

LIST OF FIGURES

CHAPTER 1

INTRODUCTION

In orthodontics, whether aligning irregular teeth or closing space after tooth extraction by sliding mechanics, a bracket bonded to a tooth slides along an arch wire as forces are transmitted to the tooth. To obtain a net load of desired magnitude, the frictional forces which develop between the brackets and the wire must be overcome by using proportionately greater forces of activation. Friction, which can exist at the interface of two solids, at a solid-fluid interface, or between fluid layers, is the resistance of one material to move tangentially with respect to another, while the two materials are in contact.

The classical model of friction analysis is shown in Figure 1 (Nikolai, 1985). In this example, a block with weight W is resting on a horizontal surface. With the application of a horizontal force, P, varying from 0 to some value to move the block, a tangential frictional force, f, will oppose the movement of the block. A normal force, N, which in this case equals W, is present, and the total force exerted by the supported surface on the block is the resultant of N and f. As P is increased, the frictional force initially resists movement of the block, until the applied force P reaches a maximum value and the block begins to move in the direction of the applied force. At this same time, the frictional force drops from a maximum f slightly and abruptly to a somewhat lower value as the static situation becomes dynamic. The region up to the point of movement is known as the range

of static friction. After movement occurs, a condition of kinetic, or sliding, friction is present. The ratio, f/N, is the coefficient of friction, μ. The endpoint of the upsloping line defines the static coefficient of friction (μ_s); the levelling off that follows defines the kinetic coefficient of friction (μ_k). Both the static and kinetic forms of sliding friction are of interest in orthodontics. Sliding friction is generated between arch wire and bracket when an arch wire is slipped through posterior tooth attachments during anterior dental segment retraction or during mesiodistal individual tooth alignments.

Previous studies measuring frictional resistance of an arch wire moving through brackets have evaluated influences of wire type, wire size, angulation, ligation force, and bracket size, although no overall understanding of the effects of surface roughness, and hardness of arch wires and brackets on friction has yet evolved. A reduction of friction between brackets and arch wires would improve the efficiency and reproducibility of force transfer during tooth movement.

NOTATION

The following symbols will be used throughout the text, tables and figures:

AES - Auger electron spectroscopy.

Co-Cr - Cobalt-chromium alloys.

f - Frictional force.

N - Normal force.

NiTi - Nickel titanium alloys.

P - Drawing force.

S.S. - Stainless steel.

β-Ti - Beta-titanium alloys.

μ - Coefficient of static or kinetic friction.

μ_k - Coefficient of kinetic friction.

μ_s - Coefficient of static friction.

LITERATURE REVIEW

Nicolls in 1968 was one of the first investigators to consider frictional forces in fixed orthodontic appliances. In a model simulating canine retraction after premolar removal, an arch wire, ligated to a horizontally positioned bracket, was attached to a dynamometer. Frictional forces increased as bracket width or wire to bracket angle increased. Ligation with an 0.25mm wire also increased friction, if the wire was tightly tied. Nicolls speculated some reduction of friction in the mouth due to the lubricating effect of saliva.

An intensive study concerning the force necessary to overcome friction and coefficients of friction was published by Andreasen and Quevedo in 1970. Frictional resistances for combinations of arch wires and brackets were evaluated under both dry and wet conditions. A force measuring apparatus representing a first premolar extraction case measured friction values as a bracket slid over an arch wire. To deliver a constant ligature force, a coil spring maintained light force between arch wire and bracket. They concluded that teeth could be moved most rapidly via translatory methods by using smaller diameter wires which decrease frictional forces and allow freedom of movement between wire and bracket slot, and by moving teeth in such a manner that the angle between wire and bracket is decreasing during tooth movement. Although these factors allow teeth to be moved rapidly, considerable tooth tipping can occur. They also found the forces affecting movement were insignificant between wet and dry conditions.

Frank and Nikolai published a paper in 1980 which addressed the levels of influence of many parameters affecting intraoral appliance friction. Again, with a first premolar extraction simulation apparatus, six independent parameters were selected for investigation: bracket size and shape, wire cross-sectional size and shape, ligature type and force, bracket/wire angulation, wire material, and interbracket distances. From their results, they concluded that without wire-bracket binding, ligature force and bracket/wire contact area are the prevailing factors. As binding between wire and bracket occurred, however, the angulation became the controlling variable. At these higher angulations, wire stiffness was influential in determining friction.

To compare the frictional forces required to overcome a simulated cuspid retraction assembly, Allai in 1984 examined 180 bracket and arch wire combinations. Three orthodontic alloys (stainless steel, nickel titanium, and beta-titanium) of two different rectangular dimensions (0.016 x 0.022 and 0.017" x 0.025") were evaluated utilizing a 0.018" Lewis bracket ligated with A-lastic ligatures. Frictional forces ranged from 55g for the 0.016" x 0.022" stainless steel to 133g for the 0.017" x 0.022" beta-titanium.

In 1986, Stannard, Gau, and Hanna conducted a detailed study to measure μ_k of 0.017" x 0.025" arch wires of four alloys against either smooth stainless steel or polytetrafluoroethylene (PTFE or Teflon) surfaces. A universal materials testing instrument applied normal forces (4-9kg) to simulate ligature ties under dry and wet (artificial

saliva) conditions. Rank orders were determined for each of the combinations tested in both the wet and dry conditions. A number of material properties were acknowledged by these investigators which might affect the coefficient of friction (yield strength, penetration hardness, Young's modulus) and different surface conditions (roughness, surface oxides). No attempt was made to determine their interrelationship except presence or absence of wear tracks after testing.

In 1988, Kusy and Whitley examined the effects of surface roughness on the coefficients of friction. Using a laser reflectometer to determine the root mean square (R.M.S.) surface roughness, polycrystalline alumina and 240 grit, 320 grit, and 1 micron polished stainless steel were tested against the four major alloy groups: stainless steel, cobalt-chromium, nickel titanium, and beta-titanium. Tested in a dry environment, μ_s and μ_k were obtained for each of the sixteen wire-contact flat combinations. Their findings were that the stainless steel alloy was the smoothest and the nickel titanium was the roughest. The stainless steel-stainless steel couple had lower μ's than even polycrystalline alumina; the beta-titanium arch wire in combination with any of the flats proved the highest. In this model, all μ's for a given wire alloy were comparable despite the flat's roughness, suggesting that low surface roughness does not correlate with the coefficient of friction.

Kusy and Whitley (1988) also investigated the effects of sliding velocity on the coefficients of friction. They tested the four major orthodontically used alloy groups against 400 and 600 grit stainless

steel flats in dry conditions, varying the relative velocity at rates from 10 mm/min to 0.0005 mm/min. They found μ_s and μ_k for stainless steel and nickel titanium invariant despite relative velocity; while a slight increase and a definite decrease of both coefficients occurred for the cobalt-chromium and the beta-titanium arch wire products, respectively.

More recently, Kusy and Whitley (1989) reported another study detailing the coefficients of friction on stainless steel and polycrystalline alumina brackets. Again the same four major alloy groups were examined against 0.018" and 0.022" stainless steel and polycrystalline alumina brackets. When the various arch wire-bracket combinations were pressed against 0.010" stainless ligature wires under dry conditions, the rankings of the coefficients of friction were stainless steel (lowest), cobalt-chromium, nickel titanium, and beta-titanium (highest). These group trends compared very favorably to all their previous work. In all cases in this study the stainless steel brackets provided smaller μ's than the polycrystalline alumina.

A reduction in the coefficient of friction between brackets and arch wires would increase the efficiency of wire movement within the bracket for tooth alignment. Past research has been directed toward producing new coatings and different wire products to reduce the coefficient of friction. In 1979 Greenberg and Kusy coated orthodontic arch wires with a polymer composite and a PTFE based coating. Respective values for μ were 0.073 and 0.028 as compared to 0.162 for uncoated wires. These preliminary results suggested that a surface coating could result in at least a 15 percent increase in force

transmission. The low standard deviations obtained further suggested that the force transmission would be more reproducible. Unfortunately, the surface coatings tended to crack on bending, reduce dimensional tolerances in the bracket slots, and sometimes stain or peel-off.

The recent literature demonstrates that ion implantation can alter surface properties of metals, significantly reducing wear and friction between contacting surfaces (Sioshansi, 1987). Ion implantation of energetic nitrogen ions into the surface of Ti-6Al-4V alloy used for hip and knee replacements can significantly reduce wear on both the metal and the ultra high molecular weight polyethylene (UHMWPE) bearing surfaces (Sioshansi et al, 1985). This in part can be explained in terms of a much lower coefficient of friction of the ion implanted surfaces.

Ion implantation is a process by which almost any element can be injected into the near-surface region of a solid by means of high-velocity ions, generally tens to hundreds of kilovolts (keV) in energy, striking a target mounted in a vacuum chamber (Figure 2). The implanted layer is shallow, varying from 0.01-1μm in the host material as a result of losing energy during collisions with substrate ions. The depth to which ions penetrate can be calculated from well established theoretical considerations. The result of ion implantation into materials is the formation of a surface alloy of graded composition that possesses no well-defined interface with respect to the substrate, as do other techniques.

Ion implantation produces surface alloys that have a number of distinct advantages. The technique can be used to coat a bulk material with a desirable alloy surface without sacrificing any of the bulk material properties. The technique can be carried out at low temperatures and the resulting surface layer is continuous with the bulk material. There are no adhesion problems since there is no interface between layers. There are no dimensional changes, and the process, carried out in a vacuum, is clean, highly reproducible, and controllable. Furthermore, since the alloys are formed by the penetration of high-velocity ions into a solid surface, the restrictions that derive from equilibrium phase diagrams do not apply to surface alloys produced by ion implantation. Drawbacks to these many advantages are the facts that ion implantation still requires relatively expensive, sophisticated equipment, that it is primarily a line-of-sight process, and that the treated layers are very shallow.

The resulting ion implanted layer has a two-fold effect on the properties and structure. First, the alloys or compounds formed by the implanted ions and substrate elements can be considerably harder than the bulk material. In general, hardened surfaces have a lower coefficient of friction than untreated materials (Pethica et al, 1983). Second, the impingement of ions with energies in the keV range make significant changes in the crystalline morphology of the surface to the extent that, and in some cases, the ion implanted surfaces become amorphous. Surface asperities, which contribute to friction, can be significantly modified, and lower values in the coefficient of friction can result.

In 1973 Hartley et al published the first friction tests carried out on implanted surfaces using a simple slow-speed sliding apparatus. A variety of ions (Sn, In, Ag, Pb, Mo) were implanted in doses in excess of $10^{16}/cm^2$ at energies typically 120keV. Macroscopic changes in friction coefficients occurred, and the majority of implanted ions decreased μ. In more recent years, numerous reports from materials science research have indicated that steels implanted with Ti (Singer and Jeffries, 1984a,b; Dillich et al, 1984; Sioshansi and Au, 1985), Ti + N (Singer and Jeffries, 1984b), Ti + C (Sioshansi and Au, 1985; Pope et al, 1984; Follstaedt et al, 1984), and Cr (Iwaki, 1987) have decreased the coefficients of friction. Additionally, ion implantations with N and C have demonstrated sharp reductions of friction and wear for Ti alloys (Oliver et al, 1984).

PURPOSE

A decrease in friction between orthodontic brackets and arch wires would improve force transmission during tooth movement, leading to more efficient, reproducible transfer. Thus, the effects of implanting various ion species into bracket models were investigated with the frictional relationship between these models and various alloys assessed.

CHAPTER 2

MATERIALS AND METHODS

General

To test the effects of ion implantation, a model system was developed with stainless steel flats, simulating orthodontic brackets, tested against four alloys. This investigation implanted various ion species into simulated stainless steel brackets. Pre- and post-implantation effects were assessed for surface chemistry, roughness and microhardness. Coefficients of friction were measured for combinations of these bracket models and arch wires.

Test Specimens

Serving as bracket models, type 304 stainless steel flats (d x h = 1/4" x 1/2", right hand cylinders, Figure 3) were end polished to a 320 grit finish— a roughness that is typical of orthodontic bracket appliances. Additional cylinders, milled to a 1μm finish, were used for quanitative testing. The finish on all cylinders was completed using wet silicon carbide papers and standard metallographic specimen techniques (Table 1).

The arch wires represented the four major orthodontic alloy groups: stainless steel, cobalt-chromium, nickel titanium, and beta-titanium (Table 1). All arch wires were 0.018" x 0.025" except the β-Ti product which was 0.017" x 0.025". These wires were used as-received except for ultrasonic cleansing.

Prior to any testing or surface modification the relative surface roughness of the wires and flats were measured for qualitative indication of surface texture using a helium-neon laser reflectometer* (Konishi et al, 1985). The technique compares the reflected light intensity from both diffuse and specular reflection. Generally, a higher surface roughness yields a more diffuse scattering of the laser beam, and a higher coefficient of friction. This test provided a baseline for surface roughness of all these tested samples. All samples (flats and arch wires) were prepared and scanned at an incident angle of 82° as detailed by Kusy et al (1988) to verify that they conformed to the nomogram previously derived. Each sample was scanned at three separate locations to determine an average relative surface reflectance (I_X/I_O). I_X/I_O is the ratio of reflected intensity from the relatively smooth test surface and the incident laser beam.

Ion Implantation

After this preliminary surface characterization, seven ion species, energies, fluences were selected for ion implantation into the test cylinders. Research facilities (NCSU Department of Electrical Engineering and Oak Ridge National Laboratory) and commercial facilities (Spire Corporation, Bedford, MA.) carried out the seven ion implantation parameters (Table 2). Eight 320 grit cylinders, for friction testing, and two 1 micron cylinders, for quanitative testing, were implanted for each parameter. These initial conditions were based on current experience for implantation of mechanical parts. Table 3

---

* Model ML-810, Metrologic Instruments, Inc., Bellmawr, NJ.

lists the various contact flat/arch wire combinations tested. Unimplanted specimens provided controls and allowed comparisons to previous studies.

Quantitative Tests

1. Auger Electron Spectroscopy

After implantation, several quantitative tests were conducted to assess possible surface changes. One 1μm polished flat of each implanted species type was sent for Auger electron spectroscopy** evaluation. In Auger electron spectroscopy (AES) an electron beam is used to excite the electronic states of the surface atoms of a solid (Figure 4). When the atoms decay from the excited state, Auger electrons are emitted carrying information that makes it possible to identify the composition of the solid surface. This analysis verified implantation and provided an in-depth compositional profile of selected surface elements.

2. Surface Roughness

To ascertain any changes in surface roughness between pre- and post-implantation, implanted cylinders were randomly selected by lot and evaluated as previously described using the laser reflectometer to determine their relative surface reflectance. These new values were then compared with the unimplanted values using paired t-tests at the 0.05 level of significance.

** JAMP-30 Auger Microprobe, JOEL, Tokyo, Japan

3. Microhardness

Also as a screening procedure to test the effect after ion implantation, a Kentron hardness tester*** was used on random 1μm implanted samples. A control along with a sample from each implanted parameter was evaluated using a Knoop indenter (Figure 5). Each sample was evaluated four times at loads of 2, 5, 10, 15, 20, 30, 40, and 50g. With the length of the indention and the known load, an average Knoop hardness number (HK) was determined for each specimen at each load from the equation:

$$HK = 14.229F/D^2$$

F = applied load in kgf

D = measured length of the long diagonal in mm

Friction Testing

A friction tester (Greenberg and Kusy, 1979) measured the coefficients of friction between bracket models and arch wire materials. The apparatus utilized with the laboratory Instron Universal Testing Machine**** (Figure 6), measures the coefficients of static and kinetic (sliding) friction. In this apparatus a spring transmits the normal force via a moveable piston to the platens (prepared flats) which are in contact with the arch wire surfaces. The magnitude of the normal force (N) was measured by means of a calibrated force transducer (T_N). The millivolt output was monitored with a high impedance recorder. The flats were drawn at a rate of 1cm/min by the

*** Kentron Microtester, Kent Cliff Labs, Peekskill, NY

**** Instron Corporation, Bedford, MA

screw driven Instron, along the gripped archwire, which was secured to the machine's load cell transducer (T_P). The millivolt signal from the drawing force transducer was digitally stored at a rate of ten data points per second. A Commodore 64 computer, interfaced with the Instron machine through an analog to digital (A-D) converter was used as a buffer to collect and store raw data. The software for the Commodore allowed for input monitoring and diskette storage functions. Coefficients of friction were measured at five normal loads for each sample combination: 200, 400, 600, 800, and 1000g. The test chamber was maintained at 34°C via a thermocouple probe. All tests were conducted under wet conditions using saliva collected from the investigator. The Instron, using a 500kg load cell, was calibrated at two load values prior to testing, rebalanced after each normal load run, and then recalibrated at the end of the day's testing.

After testing was completed, the digital data was transferred to an IBM PC/XT for analysis. From the drawing force (P) versus distance trace (Figure 7) for each combination taken from the Instron hard copy, the maximal initial force rise, which represents the static frictional force, was determined. A basic software program, <TRANSFER>, evaluated the static and kinetic coefficients of friction. By positioning cursors on the screen (Figure 8) and entering static force and normal force millivolt values, the static and kinetic coefficients of friction were calculated for all five normal force loads of each tested combination, with a unique file established for them.

The <TRANSFER> software utilized the following equation in determining the coefficients of friction:

μ = (P/2)/N, which results from the freebody diagram (Figure 9)

μ = static or kinetic coefficient of friction

P = drawing force (kg)

N = normal force (kg)

Although the coefficient of friction is independent of contact area, the reactions at both wire surfaces must be taken into account, and thus a factor of "2" enters the equation.

These unique friction files were then formatted and transferred to an Epson QX-10. Upon establishing the Epson files, linear regressions were determined for each unique data file using the program named <STAT>. The output of this program provided both a static and kinetic friction coefficient along with their respective correlation coefficients. A plot for each static and kinetic coefficient file was generated from these linear regressions via <EPPLOT>, in which the line's slope equalled μ_s or μ_k.

CHAPTER 3

RESULTS

Preliminary Results

During the early stages of this project before the aquisition of the implanted cylinders, surface modification via sputter coating was accomplished in a different approach to reduce the coefficients of friction. Coatings were chosen for their traditional improvement of wear resistance. In this experiment, S.S. cylinders were sputter coated with a 1μm thick film of Al_2O_3 + TiC, Al_2O_3, and TiB_2. These cylinders were tested as previously described against the four major orthodontic alloy groups. The μ_s and μ_k's along with their correlation coefficients are reported in Table 4. Of the tested combinations, only the Al_2O_3 + TiC film on β-Ti improved the μ_k, from 0.312 to 0.182. No other improvement was seen for any other arch wire group when compared to the S.S. control.

Quantitative

1. Auger Electron Spectroscopy

Using AES, the depth profiles for the seven ion implantations are shown in Figures 10 - 13. Figures 10 and 11 describe the data in raw intensity of peak to peak units for selected elements, and Figures 12 and 13 describe the data in concentration by atomic percent. Review of the analyses do reveal the increased presence of each of the implanted ions within the substrate surface. In all cases, iron was revealed as

the primary constituent of the bulk material. However, in all the Ti+ implantations there was a decrease in the Fe intensity during peak levels of Ti+ intensity as seen in Figures 10 and 11.

For all implantations, except carbon, the surface ion concentrations gradually increased to maximum levels at depths ranging from 35nm to 200nm and then tapered off towards zero at a 300nm depth. All distributions reveal the maximum implantation was located below the immediate surface of the implanted flats and ranged from 35-250nm. For two of the carbon implantations (C+ and N+/C+), the carbon concentration was abnormally high initially, and then decreased sharply initially taking on a Gaussian distribution pattern similar to the other implantations.

2. Relative Surface Roughness

Visual inspection of all cylinders after modification did not reveal any obvious surface alterations. Paired t-tests for surface roughness of the implanted samples (Table 5) revealed significant differences between the pre- and post- C+ and C+/N+ implanted surfaces at the 0.05 level of significance. All other tested cylinders showed no significant differences.

3. Microhardness

Microhardness measurements (Figure 14) using a Knoop tester for loads ranging from 2g to 50g, indicated an increase in hardness for the N+ and N+/Cr+ implanted cylinders, with the greatest difference seen for loads of 5g or less. The other five implanted cylinders indicated

a decrease in hardness at loads less than 5g, and generally no difference at higher loads. The differences seen in microhardness which occurred at the lighter loads provided a truer picture of surface hardness changes-- even though these layers were penetrated at the lighter loads when these findings are compared with the implantation depths.

Friction Testing

Thirty-two archwire-flat permutations were tested, with each yielding f-N plots of the static and kinetic frictional forces derived from the individual force distance traces. The plots of the regressions calculated for each permutation are shown in Figures 15 - 22. Without discarding any measurements, the thirty-two values each for μ_s and μ_k as determined from the regression slopes are reported along with their correlation coefficients (Table 6). The values obtained followed similar patterns reported previously: that is, regardless of the surface, either the S.S. or the Co-Cr arch wires demonstrated the lowest μ; β-Ti was the highest; and NiTi was intermediate. With few exceptions, the S.S. control flats outperformed the modified surfaces. Generally, any improvements seen for the implanted cylinders were marginal at best.

The kinetic coefficients of friction for unmodified S.S. measured 0.163, 0.143, 0.240, and 0.312 for the S.S., Co-Cr, NiTi, and β-Ti arch wires, respectively. The ranges of the μ_k for the various arch wires against implanted cylinders were as follows: S.S. was 0.120 (N+) -

0.301 (Ti+/N+), Co–Cr was 0.138 (N+) - 0.273 (Ti+/C+), NiTi was 0.218 (N+/C+) - 0.394 (Ti+/C+), and β–Ti was 0.216 (N+/Cr+) - 0.588 (Ti+/C+).

CHAPTER 4

DISCUSSION

Quantitative Tests

1. Auger Electron Spectroscopy

Bulk AES analyses were performed on cylinders for each parameter to document the ion concentration-range distributions. As seen in all the profiles in Figures 10 - 13, the profiles are skewed toward the surface. During each survey, those ions that were implanted into the cylinder and iron were searched for with their content reported in raw intensity and atomic percent concentration. Each analysis suggests the maximum implantation concentration is some distance within the surface suggesting the actual area of contact during the friction testing may not be against the ion-rich implanted surface.

In evaluating each of the AES profiles in Figures 10 - 13, an inverse relationship holds for the presence of iron versus the implanted Ti+ ions. Without implantation, the trace for iron would a constant value. However, with each profile that includes Ti+, the iron value drops off as the Ti+ concentration increases. Once the peak concentration of Ti+ is realized, the iron increases until reaching its full value. This finding may be a deformation of the original compound, a "matrix effect", due to the implantation of Ti+, such that the Auger electrons are not readily emitted from the iron during ion bombardment.

The analyses of the C+ and N+/C+ implantations demonstrate additional C+ on the surface as seen in the sharp drop in concentration from the surface to about 50nm (lower left-hand frame of Figures 10 - 13). This finding is suggestive of carbon contamination resulting from vacuum carburization which may well have occurred during the other implantations but was not analyzed.

Two interesting findings were discovered in reviewing the AES studies. The Ti+/N+ implantation reveals more than double the N+ concentration for the other three N+ implants (upper right-hand frame of Figures 10 and 12). During the Auger analysis, Ti+ produces several peaks one of which is of the same magnitude as the N+ peak. Thus, the measurements listed for N+ for the Ti+/N+ include the values for N+ as well as Ti+. Another anomaly of the Auger analyses was the large concentration of C+ found for Ti+/C+ as compared to C+ or N+/C+ (upper right-hand frame of Figures 11 and 13). Of note with this finding was the difference in implanting facilities as listed in Table 2.

2. Surface Roughness

Although the relative surface roughness measurements were made to insure uniformity among tested specimens, differences between pre- and post-implantation were also ascertained. No apparent change was seen visually after implantations. Finding no significant differences between pre- and post-implantation was not unexpected (Table 5) since no changes to the surface is one advantage of this surface modification. The differences seen with the C+ and N+/C+ were

unexpected, since these surfaces are more reflectant, possibly a result of surface contamination with carbon.

3. Microhardness

The indentations made with the Knoop hardness tester penetrated through the implanted layers at lighter normal loads, as these layers are of submicron thickness. The depth of penetration of the Knoop tester was based on the geometry of the diamond pyramid indenter (Figure 5). The impression created by the indenter is a rhombus with one diagonal seven times the length of the other. The depth of the impression is 1/30th of the long diagonal. Knowing the length of the long diagonal, which is measured during hardness testing, the depth of penetration can be
determined by the equation:

$$D = l_f \times 1/30 \times 492\text{nm/filar}$$

$$= l_f \times 16.4\text{nm/filar}$$

D = depth in nm

l_f = length of long diagonal as measured in filars

The shallowest depth of penetration occurred with a 2g load while microhardness testing the N+ implanted cylinder. This depth was determined to be approximately 355nm, well beyond the depth of any of the implanted layers.

Therefore, the hardness of the implanted layers is difficult to measure precisely with the Knoop microhardness tester. Only an average hardness is measured as a function of normal loads, although it does

approach the value of the implanted layer at lighter loads. The N+ and N+/Cr+ implants did demonstrate an increase in hardness at loads of 5g or less. The increase in hardness for these two implants is in agreement with Iwaki's findings (1987). Using ultralight loads, Hutchings et al, 1984 found the relative hardness of N+ implanted type 304 stainless steel to be 1.25 times higher, which is the same increase seen in this study using the conventional Knoop hardness tester. In the 15-20g range, differences between implanted and unimplanted specimens were not as apparent. Future hardness testing should employ an ultralight-load indenter to more accurately ascertain the hardness of the implanted layers without penetrating the implanted layers.

No change in hardness at lighter loads (less than 5g) may imply a decrease in hardness since the surface hardness measurement is affected by the harder underlying bulk material when the softer surface layers are penetrated. Even for the N+ and N+/Cr+ specimens which were harder at lower loads, the depth of the indentation is several times deeper than the thickness of the implanted layer. This observation suggests even a thin layer with an amorphous structure containing new compounds induced by ion implantation may affect the hardness, a property often associated with improved wear and decreased coefficients of friction for many alloys.

Friction Testing

The intention of this project was to apply material science technology to improve the application of clinical orthodontics. In clinical practice, approximately 100g of force are necessary to retract

a canine tooth (Proffit, 1986). With a μ_k equal to 0.16, an arch wire loaded to 100g would transmit 84g to the tooth, with 16g lost overcoming friction. Previous results had suggested decreases in μ_k of up to 50 percent after ion implantation. This improvement would mean 92g delivered to the tooth with only 8g lost to friction after activation of an arch wire. Therefore, for a given load, this scenario would result in a 10 percent increase in force transmission. A result of this magnitude would indicate a more efficient force transfer upon activation and less force necessary for activation. This fact would also suggest less strain on anchorage, decreasing unwanted tooth movement. No changes of this extent were seen from the results of this study.

The trends encountered among the arch wire groups during friction testing generally followed those that have been previously documented (Kusy and Whitley, 1989; Kapila, 1989): stainless steel provides the lowest μ's, followed by cobalt-chromium, nickel titanium, and beta-titanium. With few exceptions μ_s generally exceeds μ_k in the results of previous studies. Although the stainless steel controls outperformed the implanted cylinders, in 50 percent of the implanted trials, μ_s was lower than μ_k regardless of the arch wire alloy. Other than a few exceptions, no improvements were made over the unimplanted controls, and in some cases the implanted specimens actually yielded higher coefficients of friction.

During earlier friction studies, Kusy and Whitley (1988a) revealed that cold welding of the β-Ti arch wire material to the S.S. flat was one cause of high coefficients of friction. Although surface

modification by ion implantation might prevent such adhesion from occurring, only the N+/C+ implantation on β-Ti improved the μ_k from 0.312 to 0.216 (Table 6). No other improvement was seen for μ_k in this arch wire group. Further examination of Table 6 reveals that any arch wire tested against a Ti+ implantation, whether alone or in combination with another ion, yielded higher coefficients of friction. In the present study, any increased presence of Ti+, whether in the arch wire or the flats, results in increased coefficients of friction.

Previous work has demonstrated that the coefficients of friction were reduced when Ti+/N+ (Singer and Jeffries, 1984b) or Ti+/C+ (Sioshansi and Au, 1985; Pope et al, 1984; Follstaedt et al, 1984) ions were implanted. These observations were attributed to the formation of an amorphous layer as well as the formation of nitrides and carbides. Many of the highly regarded friction reduction results, which were obtained in the early eighties, may have been due to carbide contamination on the surface of the implanted materials (McHargue, 1986 and Oliver, 1989). Studies conducted in the Sandia National Laboratories (Follstaedt and Meyers, 1981) revealed that ion implantation of Ti+ plus C+ into ferrous alloys causes an amorphous surface layer to form. The Sandia studies show that the amount of residual carbon in the implantation chamber is often sufficient to cause carbon amorphortization in instances where only titanium ions are later accelerated. These studies emphasize the importance of the implantation environment, a factor that could be associated with early friction improvement. Indeed, the carbon contamination may have acted as a lubricant providing a film coating.

The values of μ_s and μ_k in air for unlubricated stainless steel span a wide variation. Several years ago Bowden and Tabor (1956) reported μ_s equal to 0.60. The American Institute of Physics Handbook (1972) listed them as 0.39 and 0.31, respectively. More recently, Nordling and Oosterman (1982) quoted the ranges to be 0.15 to 0.30 and 0.15 to 0.20, respectively. These variations may be a reflection of differences in the testing methods. Pope et al (1988) reported the μ_k for S.S. in air to improve from 0.50 to 0.30 after implantation with Ti+/C+. Their testing was accomplished using a 33g normal load for a pin (hemispherical radius of 0.79mm) on a plate. The pressures at the tip of the pin (approximately 3.5 times the yield strength of the unimplanted S.S.) are tremendous when compared with the pressures at the arch wire flat interface encountered in this study. Although the coefficients of friction are considered to be independent of contact area, in this situation the concentration of force at a single point appears to yield higher coefficients of friction.

In the present friction testing system several factors may limit the actual contact of the ion-implanted-rich layer with the arch wire surface. Unlike previous ion implantation friction studies, which were conducted under dry conditions, natural saliva bathed the tested materials during the experiments to simulate oral conditions. In one study (Stannard et al, 1986), artificial saliva was found to increase the coefficients of friction for S.S., β-Ti, and NiTi compared to dry conditions. Other friction results under wet conditions are less decisive (Nicolls, 1968; Andreasen and Quevedo, 1970). The μ_k obtained

for the control cylinders were very comparable to the results of Kusy and Whitley in 1989 (0.140, 0.163, 0.331, and 0.354, respectively) for 0.021" x 0.025" arch wires drawn against 0.022" slot S.S. brackets in a dry environment. The boundary layer created by saliva may have prevented contact between the arch wires and the ion implanted layers. The saliva itself may not have acted as a lubricant, but may have increased adhesion between surfaces during movement. Further work on the effects of saliva on sliding friction are warranted.

Two additional factors may have influenced the coefficients of friction between the ion rich layer of the flat and the arch wire. Although many earlier experiments used lighter normal loads (25-50g), Pope et al (1984) reported 50 percent reduction in μ_k for loads less than 600g. In the present investigation the loads ranged from 200-1000g. In comparing the individual coefficients of friction determined for the implanted cylinders at 200g and 400g, they reflected the same values as the overall μ_k. As described earlier, the area of peak implanted ion concentration is some distance subsurface. With the present design, only five passes were made along each implanted cylinder face with no assurance that the wire would contact the exact place on the cylinder face with each pass. Thus, sufficient surface wear to reach this area is doubtful. Singer and Jeffries (1984) reported improvements in μ_k for N+ and Ti+/N+ implantations over unimplanted 304 steel using a hardened steel ball slider. Multiple passes were made with the μ_k increasing and approaching the unimplanted values by the 20th pass. Scanning electron microscopy of the wear tracks revealed that both the Ti+ and Ti+/N+ implants initially wore

less than the unimplanted surfaces, with the dual implant showing very little relative damage after the 20th pass. Under these test conditions both the friction and wear were improved by the dual implant.

In an attempt to draw an arch wire in contact with the maximal implanted levels, the Ti+/C+ implanted cylinders were milled down using 1μm alumina lapping to remove approximately 200nm. Prior to milling the cylinder, the implanted surface was indented, and the length of the long diagonal recorded. Based on the geometry of the diamond indenter (Figure 5) the following equation was used in determining the amount of suface reduction:

$$D = l_f \times 1/30 \times 492\text{nm/filar}$$

$$= l_f \times 16.4\text{nm/filar}$$

D = depth in nm

l_f = length of long diagonal as measured in filars

To remove 200nm off the surface of a cylinder, the length of the long diagonal was reduced by 12.5 filars. Through trial and error it was found that six seconds of 1μm alumina lapping would remove 200nm of surface material. This surface removal was verified by an additional AES and comparison with the original post-implantation depth profile (Figures 23 and 24) that demonstrates a shift of the Ti+ and C+ curves towards the surface.

The friction testing was repeated only with a stainless steel arch wire, chosen for its consistent performance in previous testing. The S.S. arch wires were drawn through two different sets of the remilled

Ti+/C+ implanted cylinders. The linear regression plots of this data compared to the original Ti+/C+ are shown in Figure 25. The new μ_s and μ_k obtained were 0.210 and 0.186, an improvement over the original testing (0.246 and 0.252, respectively), but still higher than the S.S. control cylinders (0.182 and 0.163, respectively).

An additional experimental technique was attempted to obtain a homogeneous surface of the implanted layers. After the initial friction tests with the Ti+/N+ implanted cylinders were completed, the implanted surfaces were then laser annealed. Subsequently, these cylinders were tested three times by drawing new S.S. arch wires drawn between pairs of these newly modified surfaces. The regression plots of the combined data along with the original Ti+/N+ plots are shown in Figure 26. The values obtained for the combined data were 0.211 and 0.210 for μ_s and μ_k, respectively. Again an improvement was seen over the original Ti+/N+ values (0.258 and 0.301, respectively), but the S.S. control values (0.182 and 0.163, respectively) were not surpassed. No quantitative chemistry tests were performed after laser annealing these cylinders. Thus, interpretation of the results is limited because of uncertainties in the degree of homogeneity achieved as well as the possibility of losing implanted ions during the annealing process exists.

CHAPTER 5

CONCLUSIONS

1. The friction tester provided an accurate, reproducible apparatus to measure the coefficients of friction between orthodontic bracket models and arch wires.

2. Other than a few marginal exceptions, no improvements were made by the implanted specimens over the unimplanted stainless steel controls during the friction testing under the present test conditions.

3. The trends encountered among the arch wire groups during friction testing followed those that have been previously documented, that is stainless steel provides the lowest μ's, followed by cobalt-chromium, nickel titanium, and beta-titanium, respectively.

4. Future work on the effects of saliva on sliding friction are warranted.

5. Improvements seen in surface properties such as hardness and wear do not necessarily correlate with lower coefficients of friction.

BIBLIOGRAPHY

Allai, W.W. 1984. A comparison of frictional forces during simulated canine retraction on a continuous edgewise archwire. Alumni Bull., I.U.S.D. Spring: 85.

American Society for Metals Handbook Committee. Metals Handbook, Vol. 8 Mechanical Testing, ed. 9, United States, 1985, American Society for Metals, 90-91.

Andreasen, G.F. and Quevedo, F.R. 1970. Evaluation of frictional forces in the 0.022 x 0.028 edgewise bracket in vitro. J. Biomech. 3: 151-160.

Bowden, F.P. and Tabor, D. Friction and lubrication, ed. 1, New York, 1956, John Wiley, 146.

Davis, L.E., MacDonald, N.C., Palmberg, P.W., Riach, G.E., and Weber, R.E. Handbook of Auger Electron Spectroscopy, ed. 2. Philadelphia, 1978, Physical Electronics Industries, Inc., p.1.

Dillich, S.A., Bolster, R.N., and Singer, I.L. 1984. Friction and wear behavior of a cobalt-based alloy implanted with Ti or N. Mat. Res. Soc. Symp. Proc. 27: 637-642.

Follstaedt, D.M. and Meyers, S.M., 1981. Ion beam modification of materials. Nucl. Instrum. Meth. 209/210: 1023-1031.

Follstaedt, D.M., Yost, F.G., and Pope, L.E. 1984. Microstructures of stainless steels exhibiting reduced friction and wear after implantation with Ti and C. Mat. Res. Soc. Symp. Proc. 27: 655-660.

Frank, C. A. and Nikolai, R. J. 1980. A comparative study of frictional resistances between orthodontic bracket and arch wire. Am. J. Orthod. 78: 593-609.

Gray, D.E. American Institute of Physics Handbook, ed. 3, New York, 1972, McGraw-Hill, 2-42 - 2-43.

Greenberg, A.R. and Kusy, R.P. 1979. A survey of specialty coatings for orthodontic wires. J. Dent. Res. 58: (Special Issue A) 98.

Hutchings, R., Oliver, W.C., and Pethica, J.B. Surface Engineering, ed. 1, New York, 1984, Saunders, Inc., 170-184.

Iwaki, M. 1987. Tribological properties of ion-implanted steels. Mat. Sci. and Eng. 90: 263-271.

Kapila, S., Angolkar, P., Duncanson, M.G.Jr., and Nanda, R.S. 1989. Effect of wire size and alloy on bracket-wire friction. J. Dent Res. 68: (Special Issue) 386.

Konishi, R.N., Whitley, J.Q., and Kusy, R.P. 1985. Surface roughness of a dental amalgam via a laser scattering test. Dent. Mater. 1: 55-57.

Kusy, R.P. and Whitley, J.Q. 1988a. Effects of surface roughness on the coefficients of friction in a model orthodontic system. In press.

Kusy, R.P. and Whitley, J.Q. 1988b. Effects of sliding velocity on the coefficients of friction in a model orthodontic system. In press.

Kusy, R.P., Whitley, J.Q., Mayhew, M.J., and Buckthal, J.E. 1988. Surface roughness of orthodontic archwires via laser spectroscopy. Angle Orthod. 58: 33-45.

Kusy, R.P. and Whitley, J.Q. 1989. Coefficients of friction of arch wires on stainless steel and polycrystalline alumina brackets: I. The dry state. In press.

McHargue, C.J. 1986. Ion implantation in metals and ceramics. Int. Met. Rev. 31: 49-76.

Nicolls, J. 1967-1968. Frictional forces in fixed orthodontic appliances. Dent. Prac. Dent. Rec. 18: 362-366.

Nikolai, R.J. Bioengineering Analysis of Orthodontic Mechanics. ed. 1, Philadelphia, 1985, Lea and Febiger, 53-56.

Nordling, C. and Oosterman, J. Physics Handbook, ed. 2, London, 1982, Chartwell-Bratt Ltd., 43.

Oliver, W.C., Hutchings, R., Pethica, J.B., Paradis, E.L., and Shuskis, A.J. 1984. Ion implanted Ti-6Al-4V. Mat. Res. Soc. Symp. 27: 705-710.

Oliver, W.C. 1989. Personal communication.

Pethica, J.B., Hutchings, R., and Oliver, W.C. 1983. Composition and hardness profiles in ion implanted metals. Nucl. Insrum. Meth. 209/210: 995-1000.

Pope, L.E., Yost, F.G., Foilstaedt, D.M., Picraux, S.T., and Knapp, J.A. 1984. Friction and wear reduction of 440C stainless steel by ion implantation. Mat. Res. Soc. Symp. Proc. 27: 661-666.

Proffit, W.R. Contemporary Orthodontics. ed. 1, St. Louis, 1986, C.V. Mosby, 236.

Singer, I.L. and Jeffries, R.A. 1984a. Processing steels for tribological applications by titanium implantation. Mat. Res. Soc. Symp. Proc. 27: 637-642.

Singer, I.L. and Jeffries, R.A. 1984b. Friction, wear, and deformation of soft steels implanted with Ti and N. Mat. Res. Soc. Symp. Proc. 27: 667-672.

Sioshansi, P. 1987. Surface modification of industrial components by ion implantation. Mat. Sci. Engineering 90: 373-377.

Sioshansi, P., and Au, J.J. 1985. Improvements in sliding wear for bearing-grade steel implanted with titanium and carbon. Mat. Sci. Eng. 69: 161-166.

Sioshansi, P., Oliver, R.W., and Matthews, F.D. 1985. Wear improvement of surgical titanium alloys by ion implantation. J. Vac. Sci. Technol. A: 3.

Stannard, J.G., Gau, J.M., and Hanna, M.A. 1986. Comparative friction of orthodontic wires under dry and wet conditions. Am. J. Orthod. 89: 485-491.

TABLES

Table 1 - Materials to be Evaluated

Contact Flats

Alloy Type	Code	Nominal Finish	Manufacturer
Stainless Steel	S.S.	320 Grit*	UNC-CH Lab
Stainless Steel	S.S.	1 micron**	UNC-CH Lab

* Grinding sequence- 240 and 320 grit carbide (wet)
** Grinding sequence- 320,400, and 600 grit carbide (wet) followed by 6μm and 1μm alumina lapping

Arch Wires

Alloy Type	Code	Size	Product
Stainless Steel	S.S.	0.018" x 0.025" (Straight)	Unitek Standard™ a
Nickel Titanium	NiTi	0.018" x 0.025" (Preformed)	Nitinol™ a
Cobalt-Chromium	Co-Cr	0.018" x 0.025" (Straight)	Yellow Elgiloy™ b
Beta-Titanium	β-Ti	0.017" x 0.025" (Straight)	T.M.A.™ c

a Unitek Corporation, Monrovia, CA.
b Rocky Mountain Orthodontics, Denver, CO.
c Ormco Corporation, Glendora, CA.

Table 2 - Ion Implantation Parameters

Substrate	Ion Implantation Parameters			
	Ion	Energy	Dose	
304 Stainless Flat	N+	60 keV	2×10^{17} cm^{-2}	a
"	Ti+	170 keV	4×10^{17} cm^{-2}	b
	N+	60 keV	2×10^{17} cm^{-2}	b
"	N+	60 keV	2×10^{17} cm^{-2}	a
	C+	60 keV	2×10^{17} cm^{-2}	c
"	N+	60 keV	2×10^{17} cm^{-2}	b
	Cr+	120 keV	3×10^{17} cm^{-2}	b
"	Ti+	170 kev	4×10^{17} cm^{-2}	b
"	Ti+	170 kev	4×10^{17} cm^{-2}	b
	C+	60 keV	2×10^{17} cm^{-2}	b
"	C+	60 keV	2×10^{17} cm^{-2}	c

a NCSU Electrical Engineering Dept, NC.
b Spire Corporation, Bedford, MA.
c Oak Ridge National Laboratory, TN.

Table 3 - Initial Screening Combinations

Contact Flat Implantation	Arch Wire Alloy S.S.	Co-Cr	NiTi	β-Ti
Unimplanted	X	X	X	X
N+	X	X	X	X
Ti+/N+	X	X	X	X
N+/C+	X	X	X	X
N+/Cr+	X	X	X	X
Ti+	X	X	X	X
Ti+/C+	X	X	X	X
C+	X	X	X	X

X = Scheduled test combinations

Table 4 - Summary of the Coefficients of Friction for Sputter Coated Flat/Arch Wire Combinations *

(wet flat velocity = 1 cm/min at a temperature of 34°C)

Contact Flat	Arch Wire Alloy							
	S.S.		Co-Cr		NiTi		β-Ti	
S.S.	0.182[a]	0.163[b]	0.124	0.143	0.343	0.240	0.360	0.312
Control	0.997[c]	0.958[d]	0.992	0.994	0.994	0.961	0.986	0.996
Al_2O_3 + TiC	0.264	0.231	0.281	0.250	0.354	0.281	0.297	0.182
	0.989	0.960	0.983	0.989	0.968	0.992	0.963	0.951
Al_2O_3	0.179	0.170	0.201	0.197	0.274	0.306	0.326	0.406
	0.923	0.957	0.997	0.914	0.972	0.967	0.887	0.981
TiB_2	0.247	0.215	0.487	0.418	0.387	0.367	0.269	0.412
	0.941	0.966	0.981	0.978	0.908	0.998	0.942	0.907

[a] Coefficients of static friction (μ_s) were based on the linear regression data of all observations.

[b] Coefficients of static friction (μ_k) were based on the linear regression data of all observations.

[c] Correlation coefficients for the μ_s ($p \leq 0.05$).

[d] Correlation coefficients for the μ_k ($p \leq 0.05$).

* Five observations were utilized to determine μ_s and μ_k.

Table 5 - Relative Surface Reflectance (RSR)

Ion Species (n=population)	Mean RSR Pre-Implant	Mean RSR Post-Implant	P-Value *
N+ (n=13)	0.413 ± (0.024)	0.425 ± (0.038)	0.32
Ti+/N+ (n=8)	0.445 ± (0.022)	0.450 ± (0.016)	0.16
N+/C+ (n=8)	0.422 ± (0.016)	0.431 ± (0.018)	≤0.0094
N+/Cr+ (n=8)	0.393 ± (0.033)	0.401 ± (0.031)	0.09
Ti+ (n=8)	0.424 ± (0.019)	0.422 ± (0.025)	0.51
Ti+/C+ (n=8)	0.413 ± (0.033)	0.417 ± (0.028)	0.49
C+ (n=8)	0.416 ± (0.019)	0.427 ± (0.019)	≤0.0056

* = Student's t-test of paired data
RSR = Relative Power (I_X/I_O) @ 82°

Table 6 - Summary of the Coefficients of Friction for Ion Implanted Flat/Arch Wire Combinations *

(wet flat velocity = 1 cm/min at a temperature of 34°C)

Contact Flat	Arch Wire Alloy							
	S.S.		Co-Cr		NiTi		β-Ti	
Unimpl	0.182[a]	0.163[b]	0.124	0.143	0.343	0.240	0.360	0.312
	0.997[c]	0.958[d]	0.992	0.994	0.994	0.961	0.986	0.996
N+	0.152	0.120	0.169	0.138	0.208	0.324	0.372	0.310
	0.931	0.921	0.985	0.950	0.981	0.995	0.960	0.977
Ti+/N+	0.258	0.301	0.278	0.264	0.366	0.394	0.599	0.330
	0.952	0.988	0.983	0.983	0.946	0.940	0.982	0.981
N+/C+	0.220	0.241	0.247	0.265	0.322	0.218	0.291	0.216
	0.999	0.982	0.981	0.984	0.920	0.993	0.969	0.939
N+/Cr+	0.245	0.261	0.294	0.231	0.384	0.281	0.323	0.331
	0.940	0.983	0.975	0.965	0.981	0.999	0.900	0.951
Ti+	0.225	0.189	0.160	0.163	0.208	0.236	0.470	0.571
	0.903	0.961	0.888	0.957	0.963	0.978	0.881	0.942
Ti+/C+	0.246	0.252	0.261	0.273	0.384	0.294	0.585	0.588
	0.964	0.987	0.992	0.997	0.952	0.998	0.989	0.960
C+	0.158	0.172	0.248	0.266	0.411	0.305	0.271	0.351
	0.960	0.988	0.989	0.971	0.974	0.951	0.956	0.926

[a] Coefficients of static friction (μ_s) were based on the linear regression data of Figures 15 - 22.

[b] Coefficients of static friction (μ_k) were based on the linear regression data of Figures 15 - 22.

[c] Correlation coefficients for the μ_s ($p \leq 0.05$).

[d] Correlation coefficients for the μ_k ($p \leq 0.05$).

* Five observations were utilized to determine μ_s and μ_k.

FIGURES

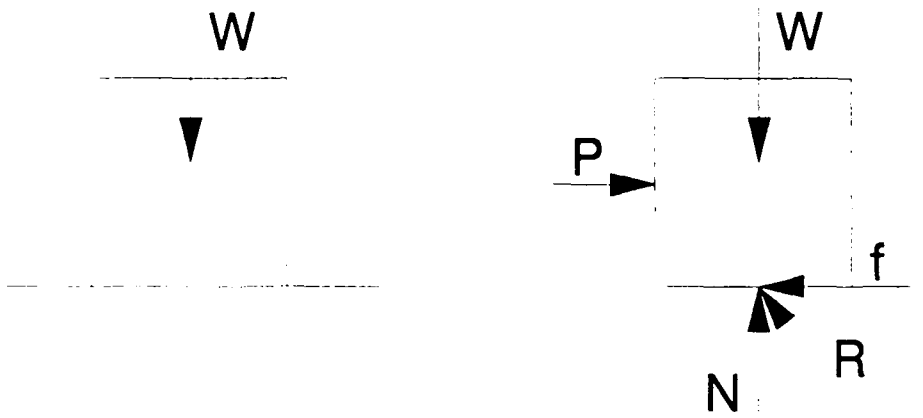

a.

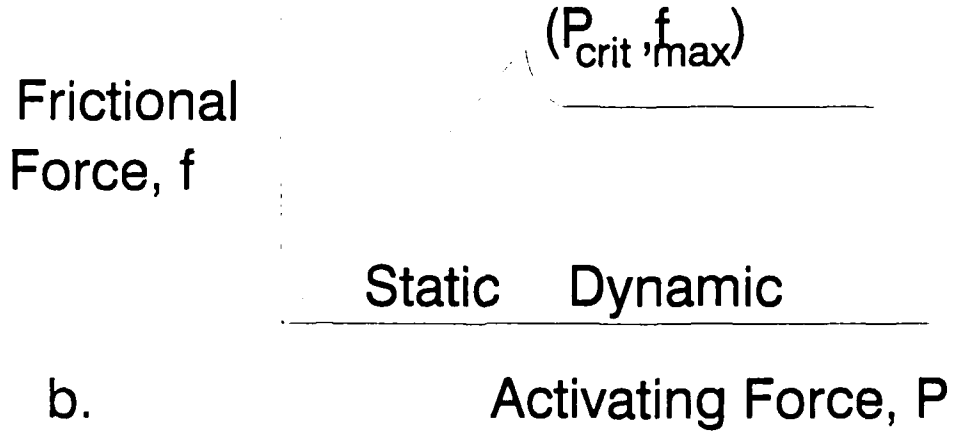

b.

Figure 1. a. Active and responsive forces exerted on a block supported by a rough horizontal surface. b. Relationship of the magnitudes of active and frictional forces, P and f, for the block and surface of (a.) above. (Redrawn from Nikolai).

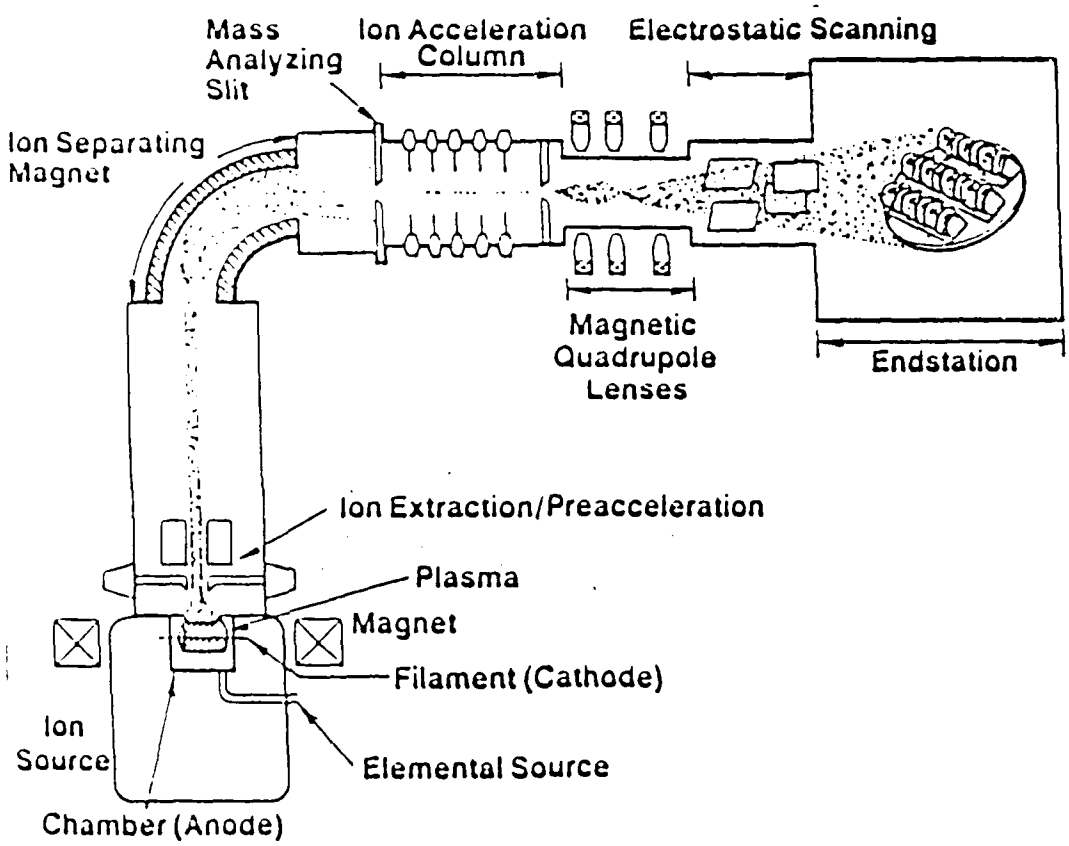

Figure 2. Schematic of an ion implantation end station. (Reprinted from Spire).

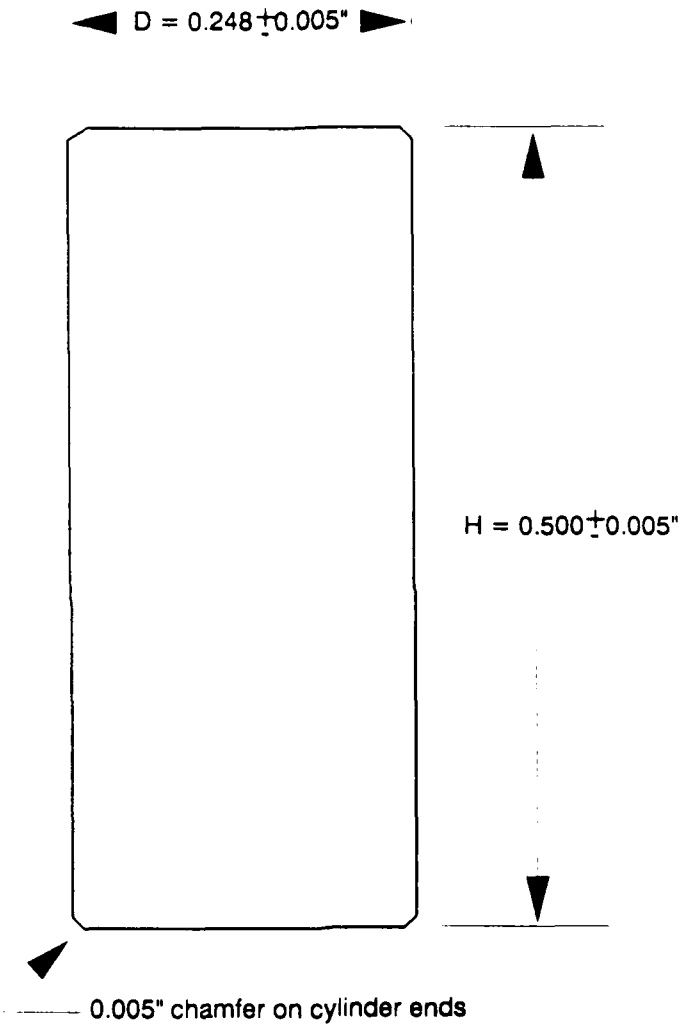

Figure 3. Test right-hand cylinders fabricated with type 304 stainless steel.

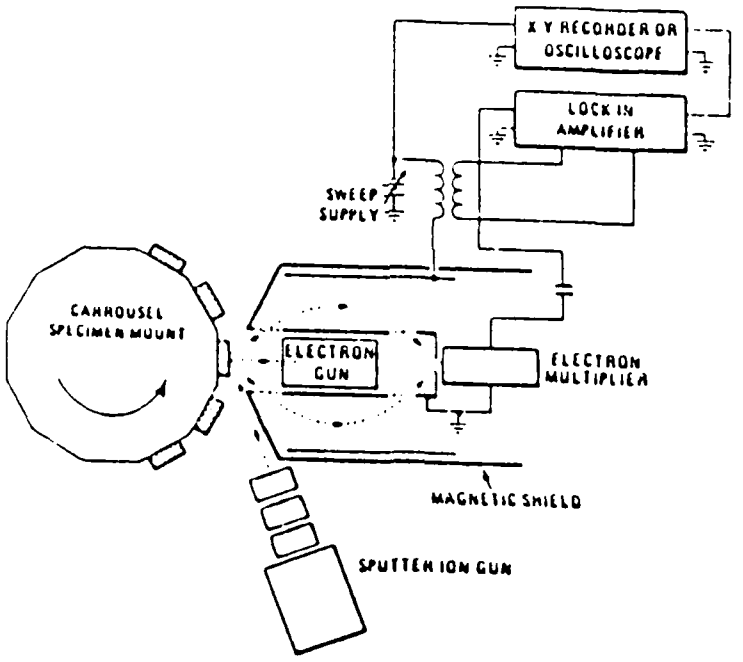

Figure 4. Schematic of arrangement used for obtaining standard Auger spectra. (Reprinted from Handbook of Auger Electron Spectroscopy)

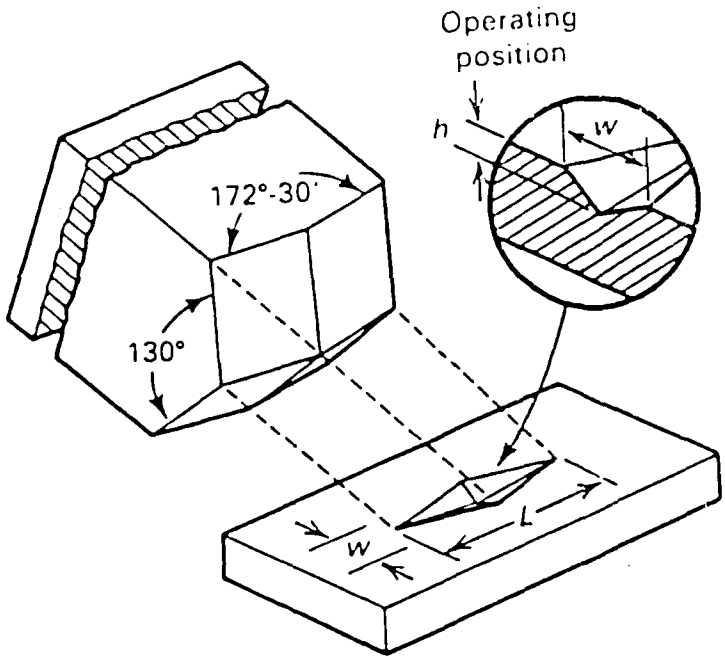

Figure 5. Pyramidal Knoop indenter and resulting indentation in the workpiece. (Reprinted from Metals Handbook)

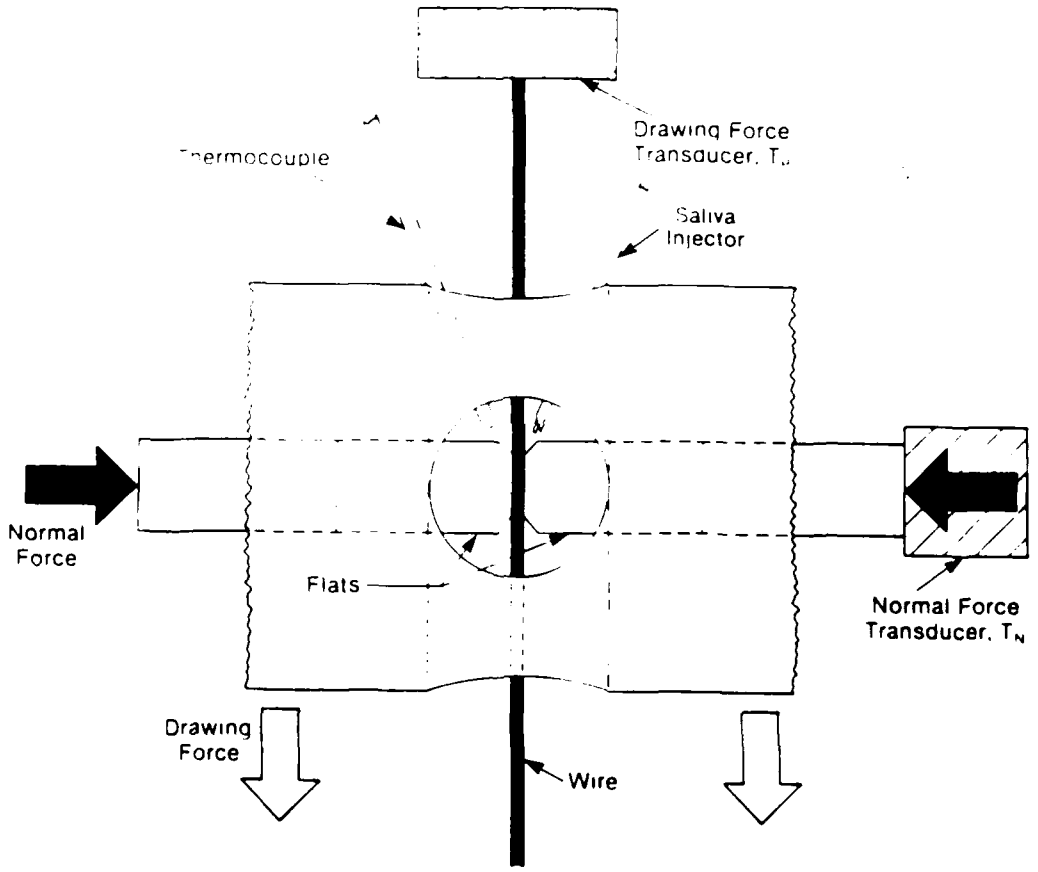

Figure 6. Diagram of the friction testing apparatus: arch wire is extending vertically through the sliding cylinders which press against the arch wire with a known force.

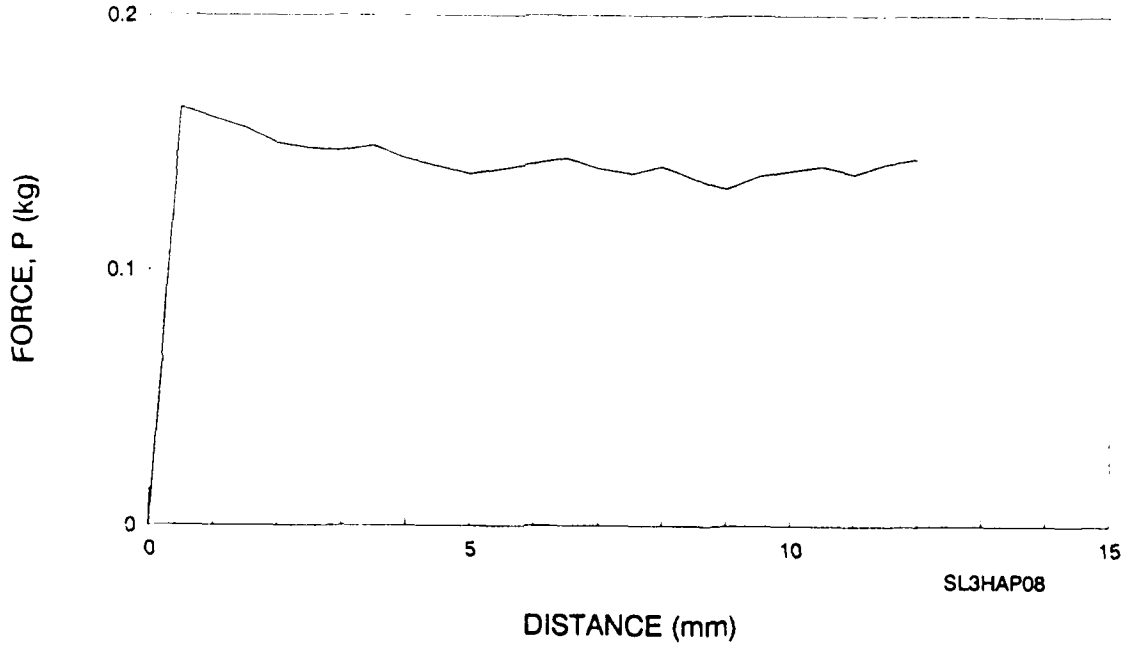

Figure 7. Representative force-distance trace of stainless steel control cylinder against a stainless steel arch wire.

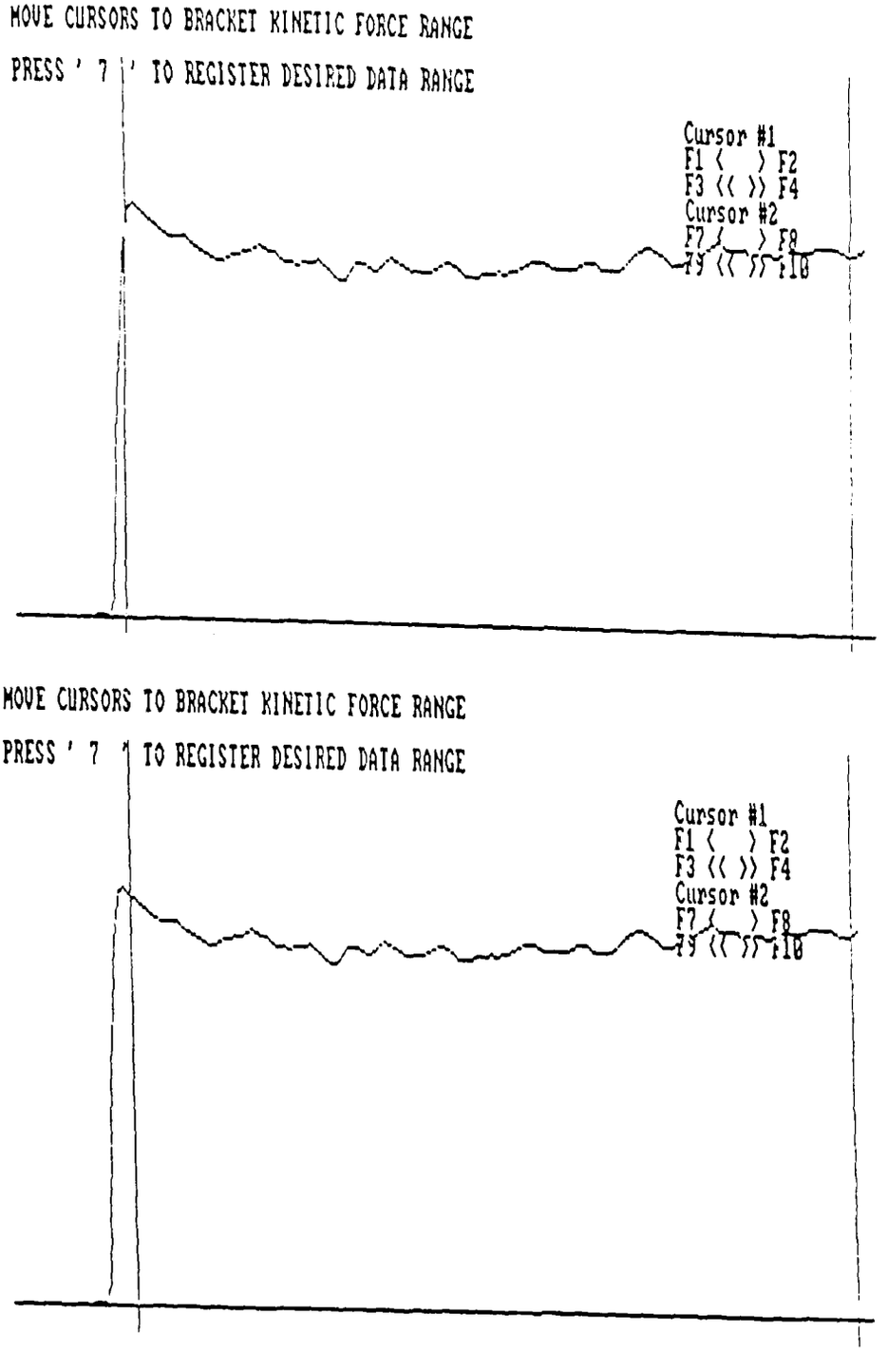

Figure 8. Two computer screens from <TRANSFER>. Top shows tracing before cursors are placed and bottom shows the two cursors positioned.

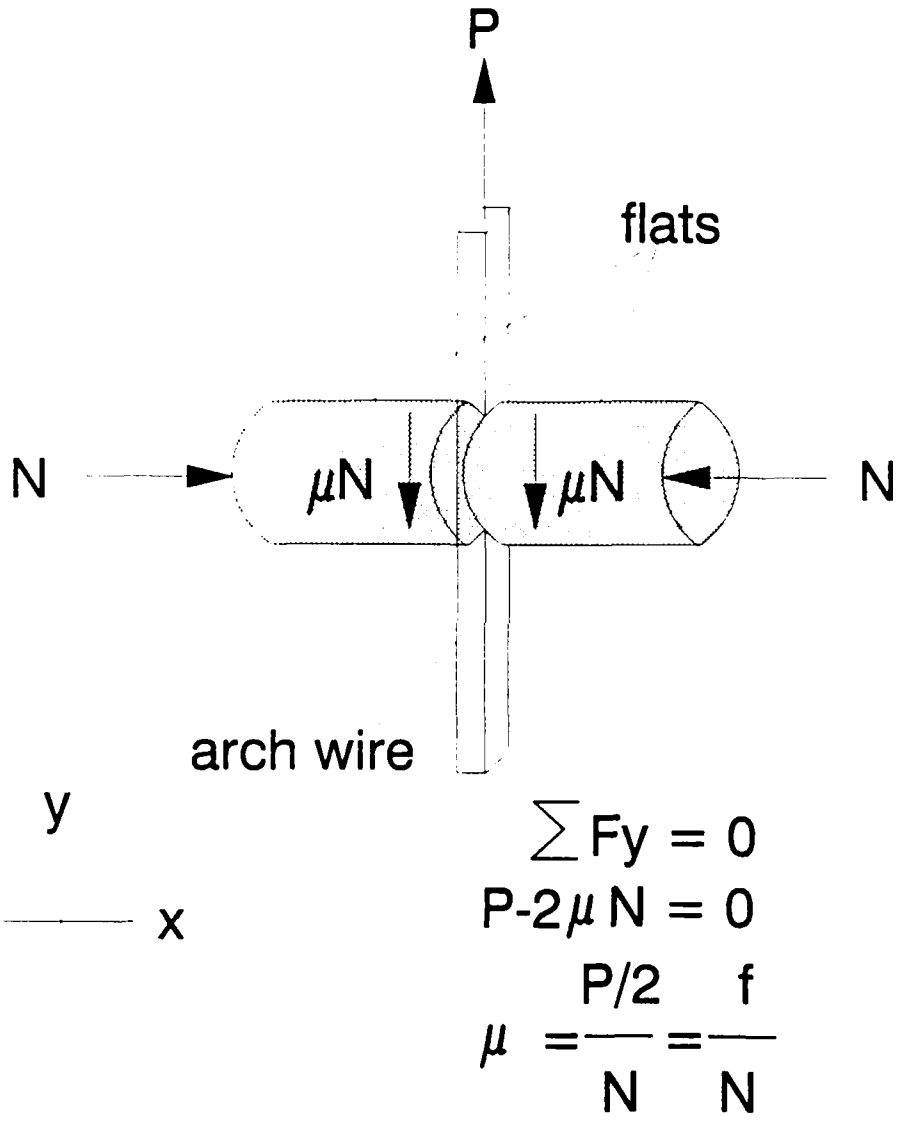

Figure 9. Free body diagram. (Redrawn from Greenberg and Kusy)

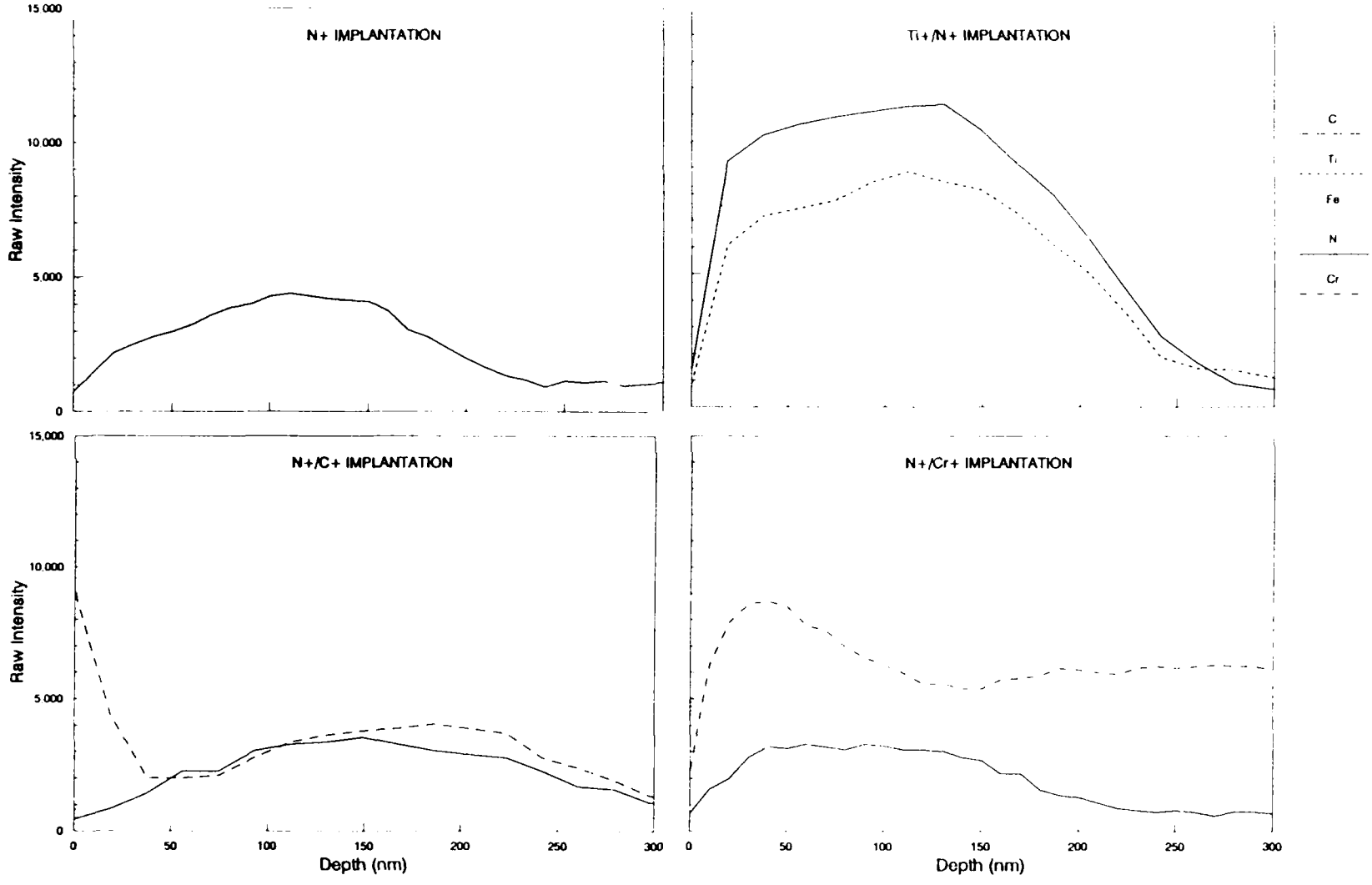

Figure 10. Auger electron spectroscopy analyses for N+, Ti+/N+, N+/C+, and N+/Cr+ implantations as reported in raw intensity.

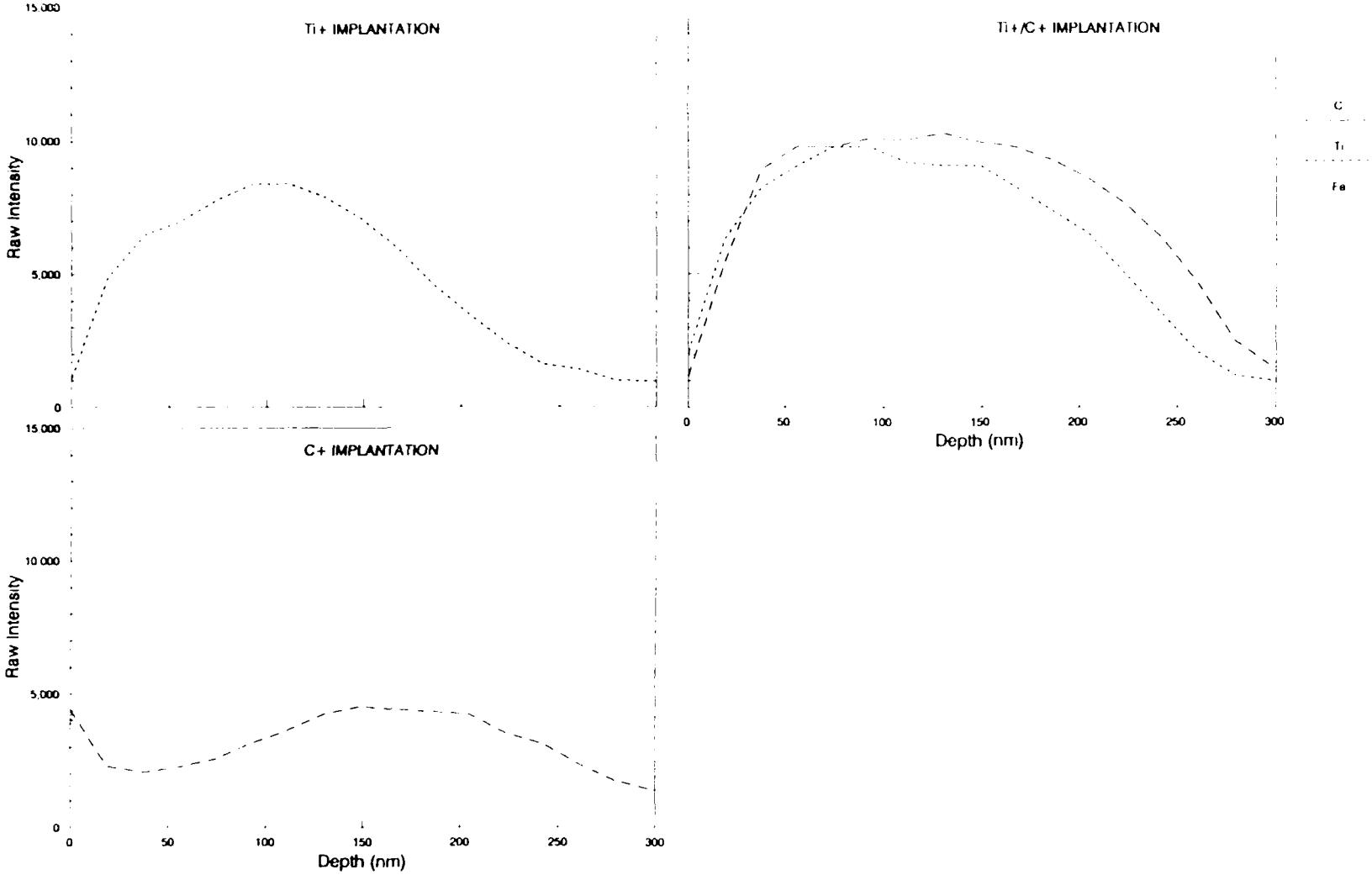

Figure 11. Auger electron spectroscopy analyses for Ti+, Ti+/C+, and C+ implantations as reported in raw intensity.

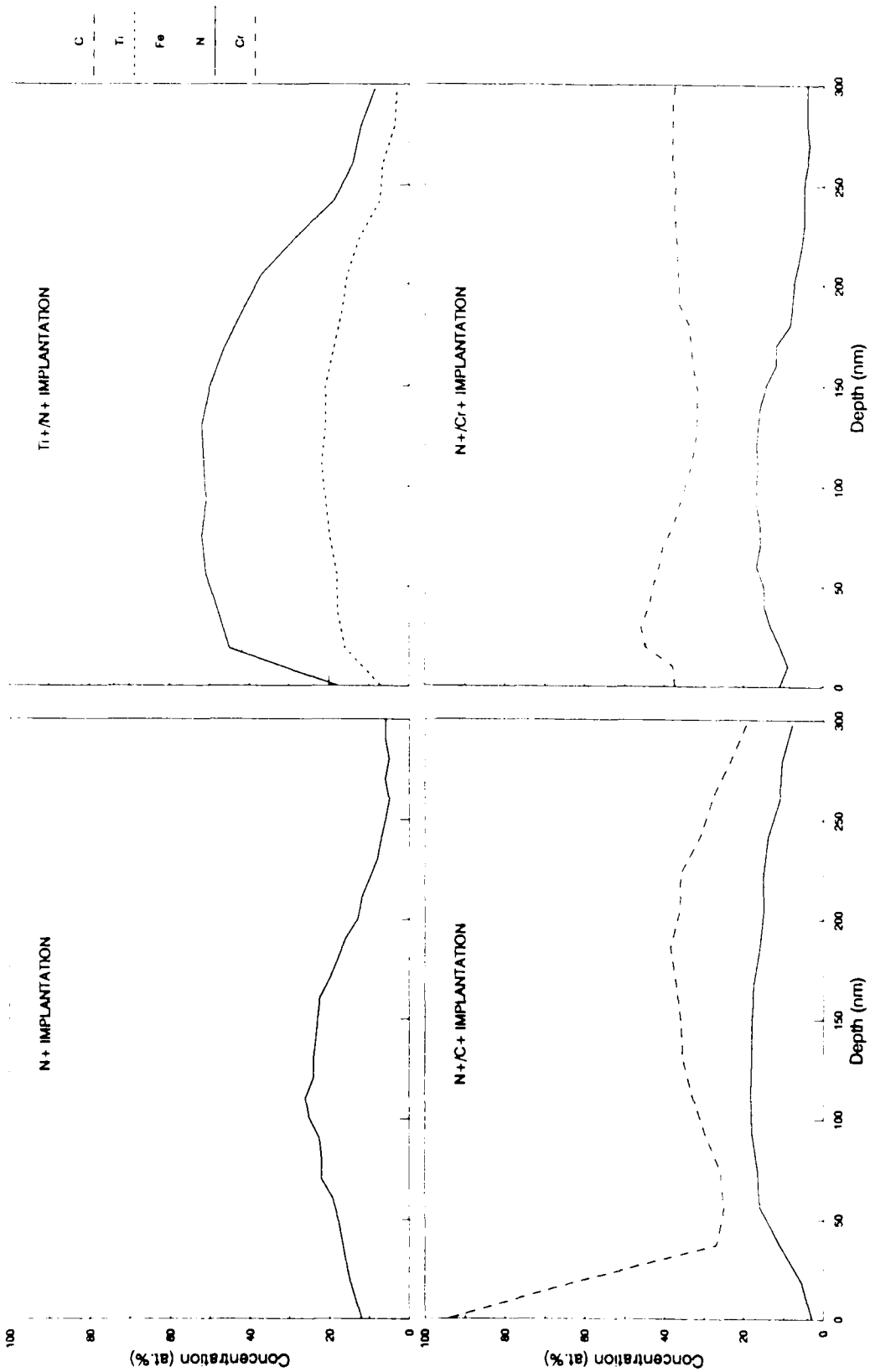

Figure 12. Auger electron spectroscopy analyses for Ar, Ti+/N+, N+/C+, and N+/Cr+ implantations as reported in atomic percent concentration.

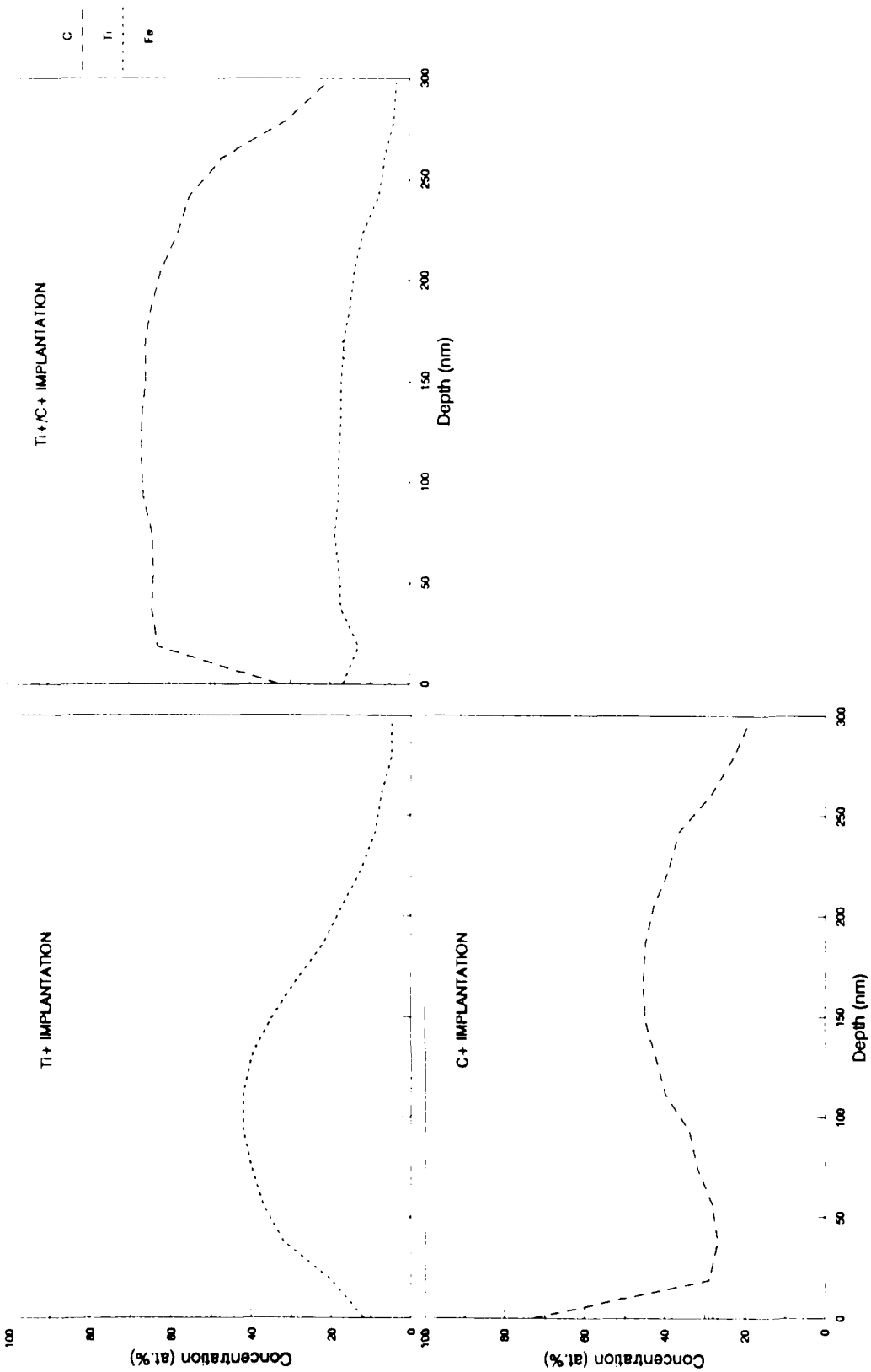

Figure 13. Auger electron spectroscopy analyses for Ti+, Ti+/C+, and C+ implantations as reported in atomic precent concentration.

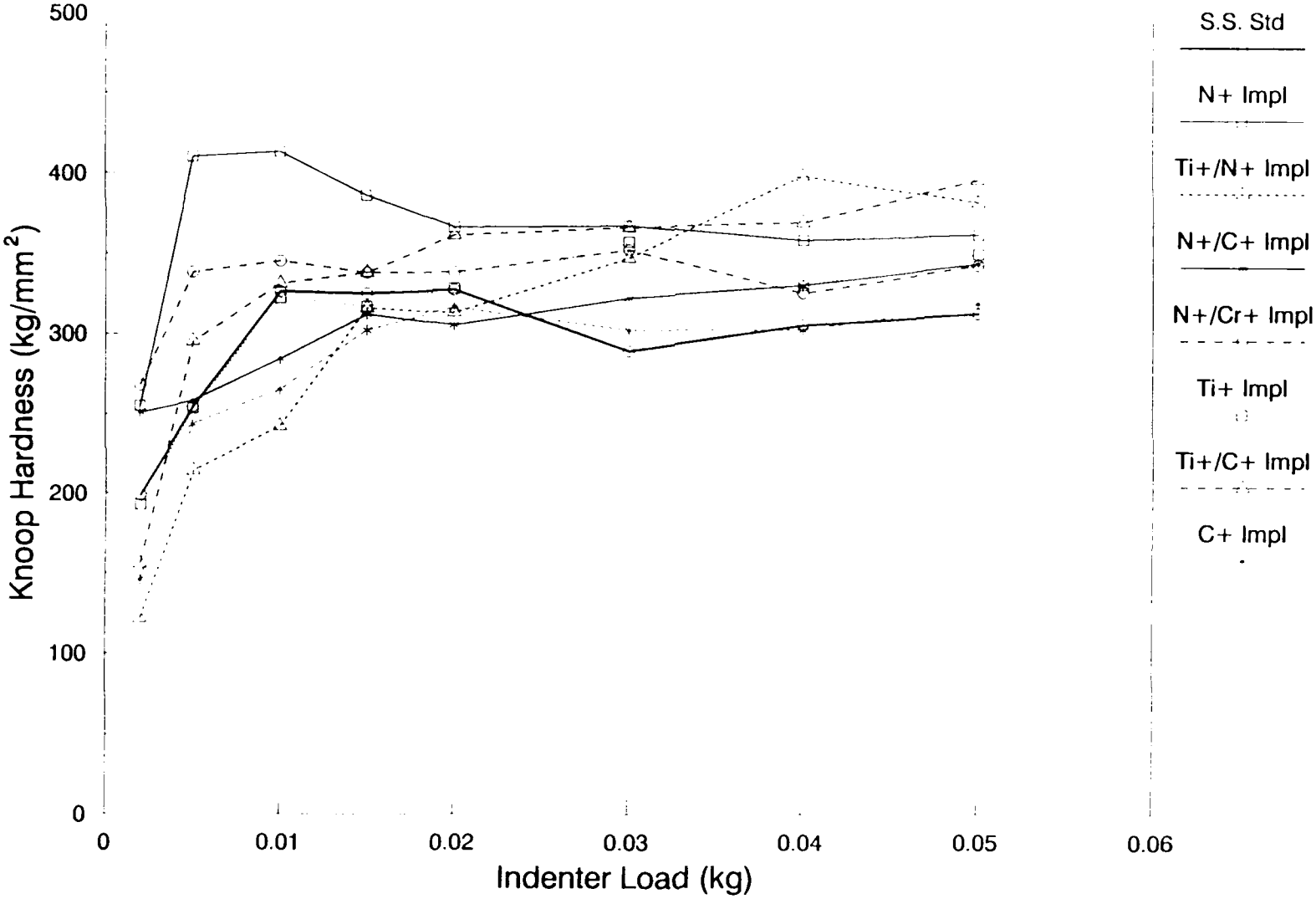

Figure 14. Results of the Knoop microhardness tests.

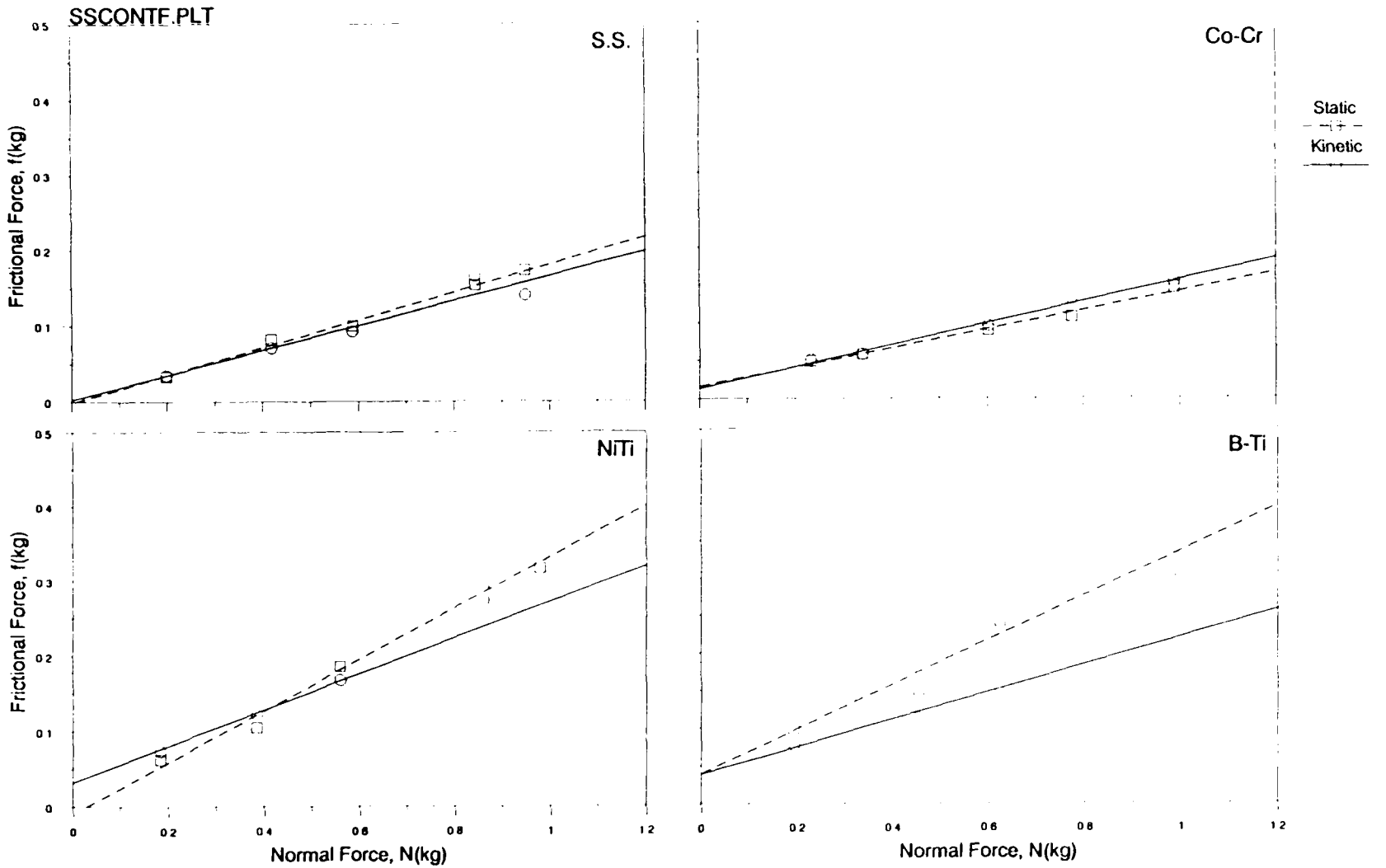

Figure 15. Plots of the frictional force (f=P/2) versus normal force (N) for stainless steel control against four arch wire alloys. Based upon the static and kinetic data which is reported in Table 6.

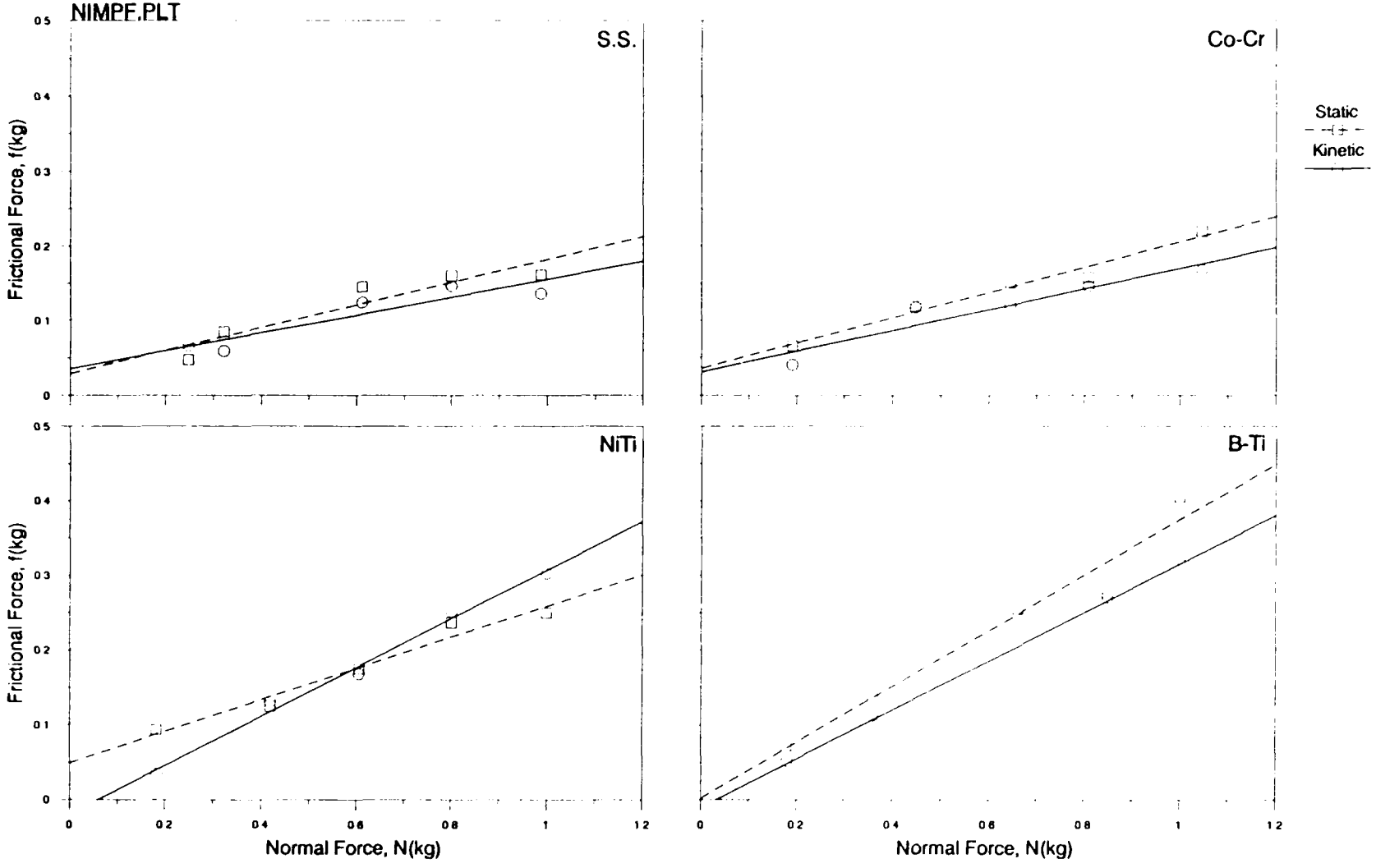

Figure 16. Plots of the frictional force (f=P/2) versus normal force (N) for N+ implanted stainless steel against four arch wire alloys. Based upon the static and kinetic data which is reported in Table 6.

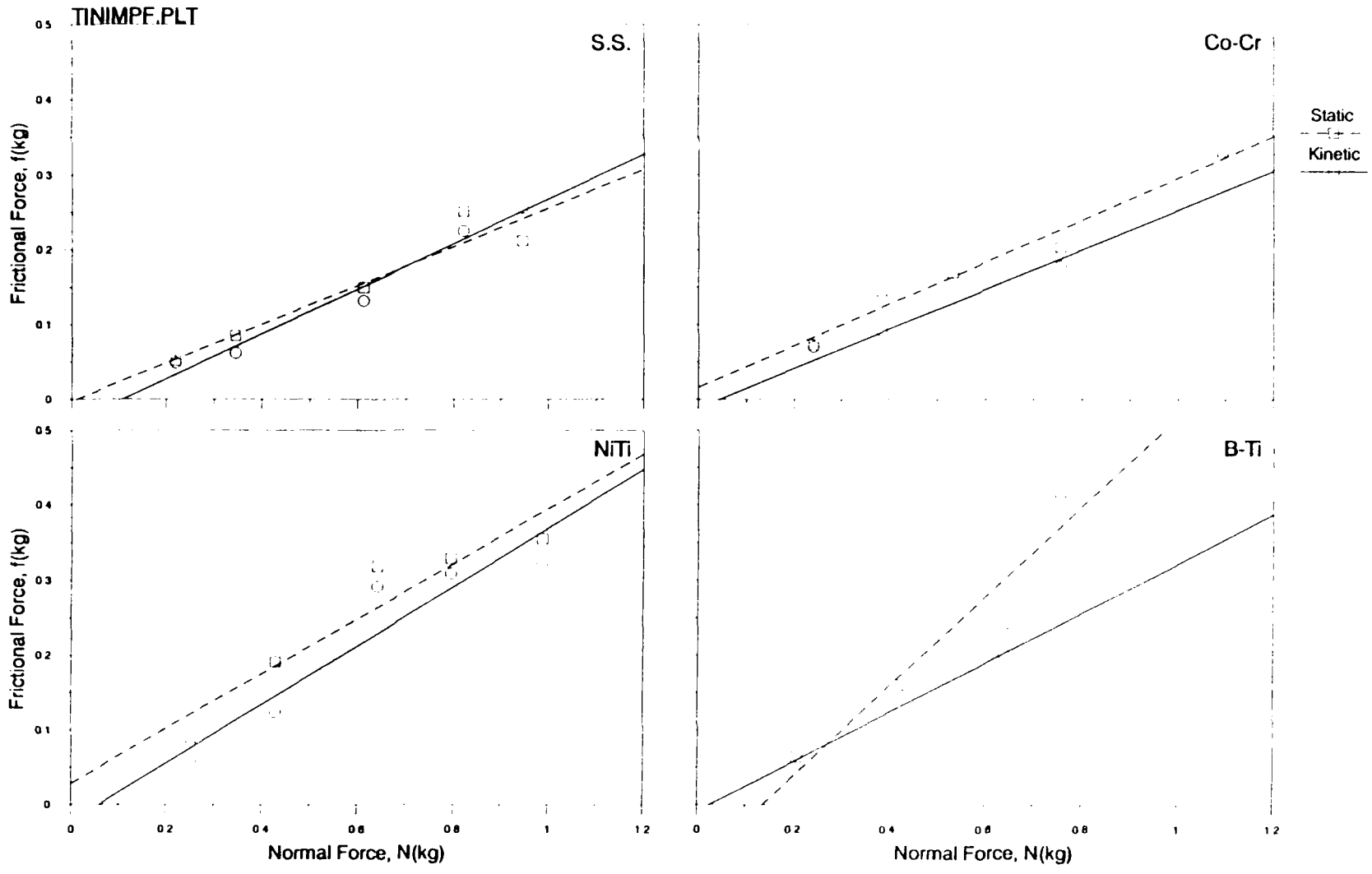

Figure 17. Plots of the frictional force (f=P/2) versus normal force (N) for Ti+/N+ implanted stainless steel against four arch wire alloys. Based upon the static and kinetic data which is reported in Table 6.

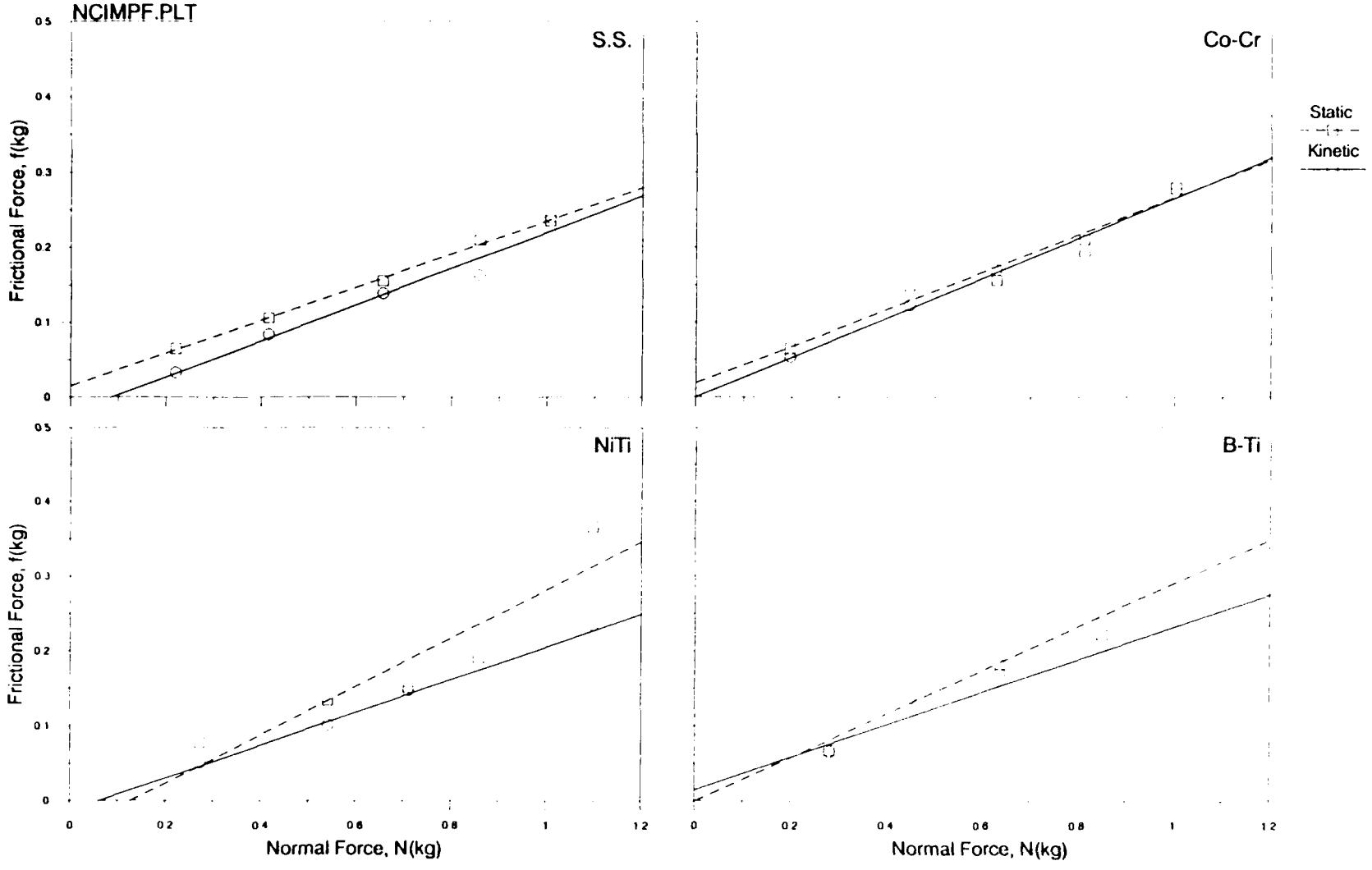

Figure 18. Plots of the frictional force (f=P/2) versus normal force (N) for N+/C+ implanted stainless steel against four arch wire alloys. Based upon the static and kinetic data which is reported in Table 6.

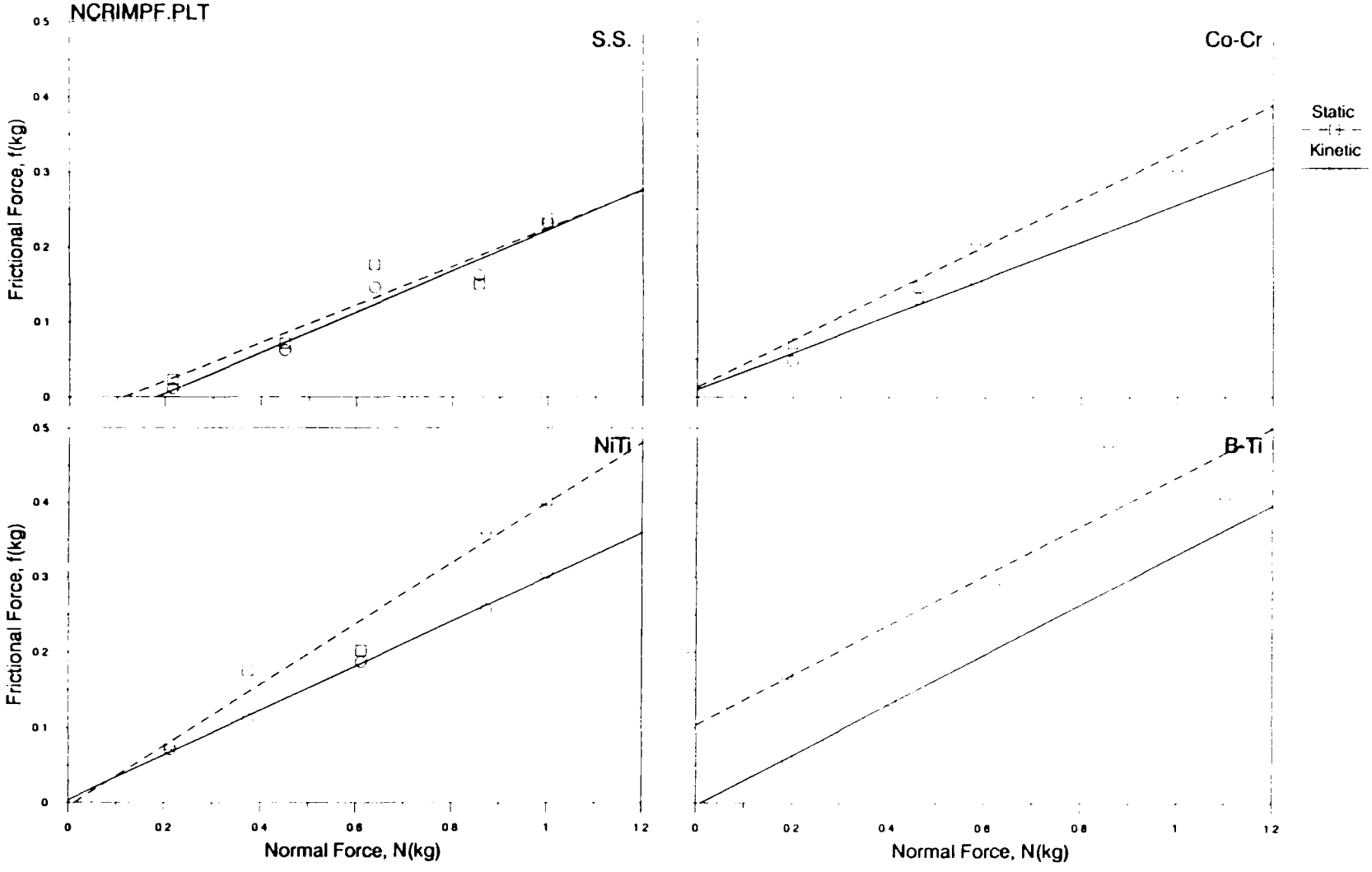

Figure 19. Plots of the frictional force (f=P/2) versus normal force (N) for N+/Cr+ implanted stainless steel against four arch wire alloys. Based upon the static and kinetic data which is reported in Table 6.

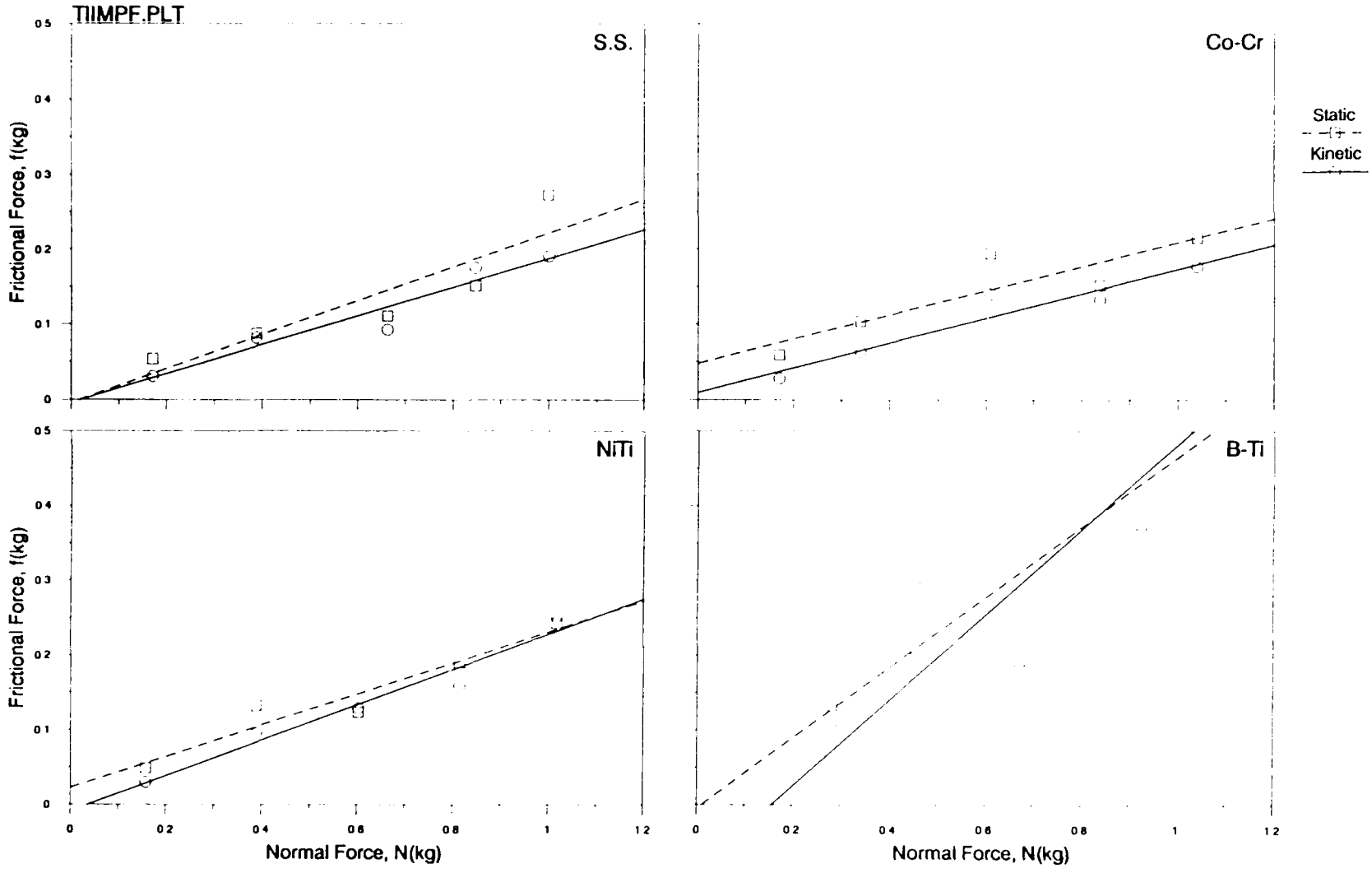

Figure 20. Plots of the frictional force (f=P/2) versus normal force (N) for Ti+ implanted stainless steel against four arch wire alloys. Based upon the static and kinetic data which is reported in Table 6.

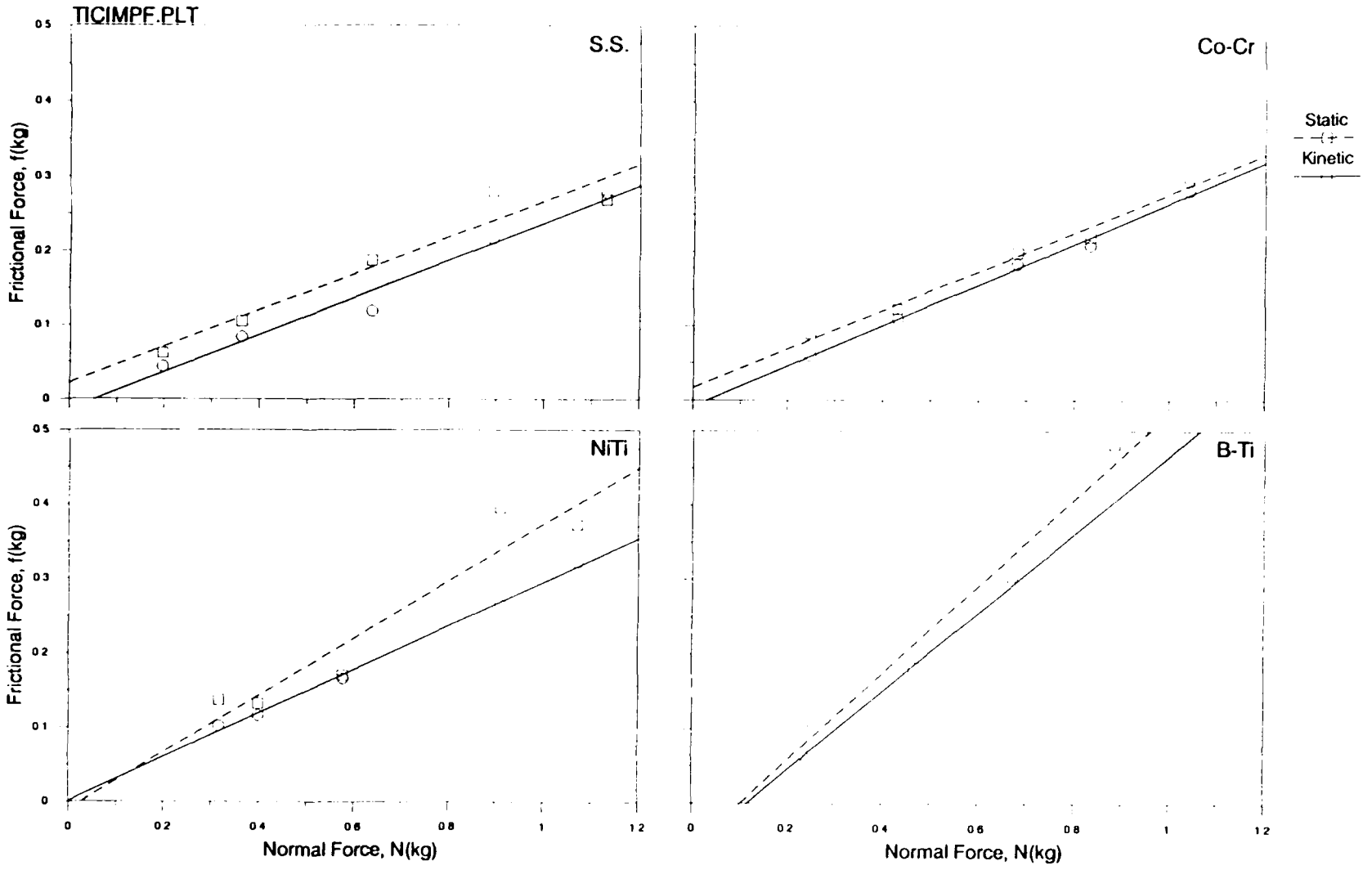

Figure 21. Plots of the frictional force (f=P/2) versus normal force (N) for Ti+/C+ implanted stainless steel against four arch wire alloys. Based upon the static and kinetic data which is reported in Table 6.

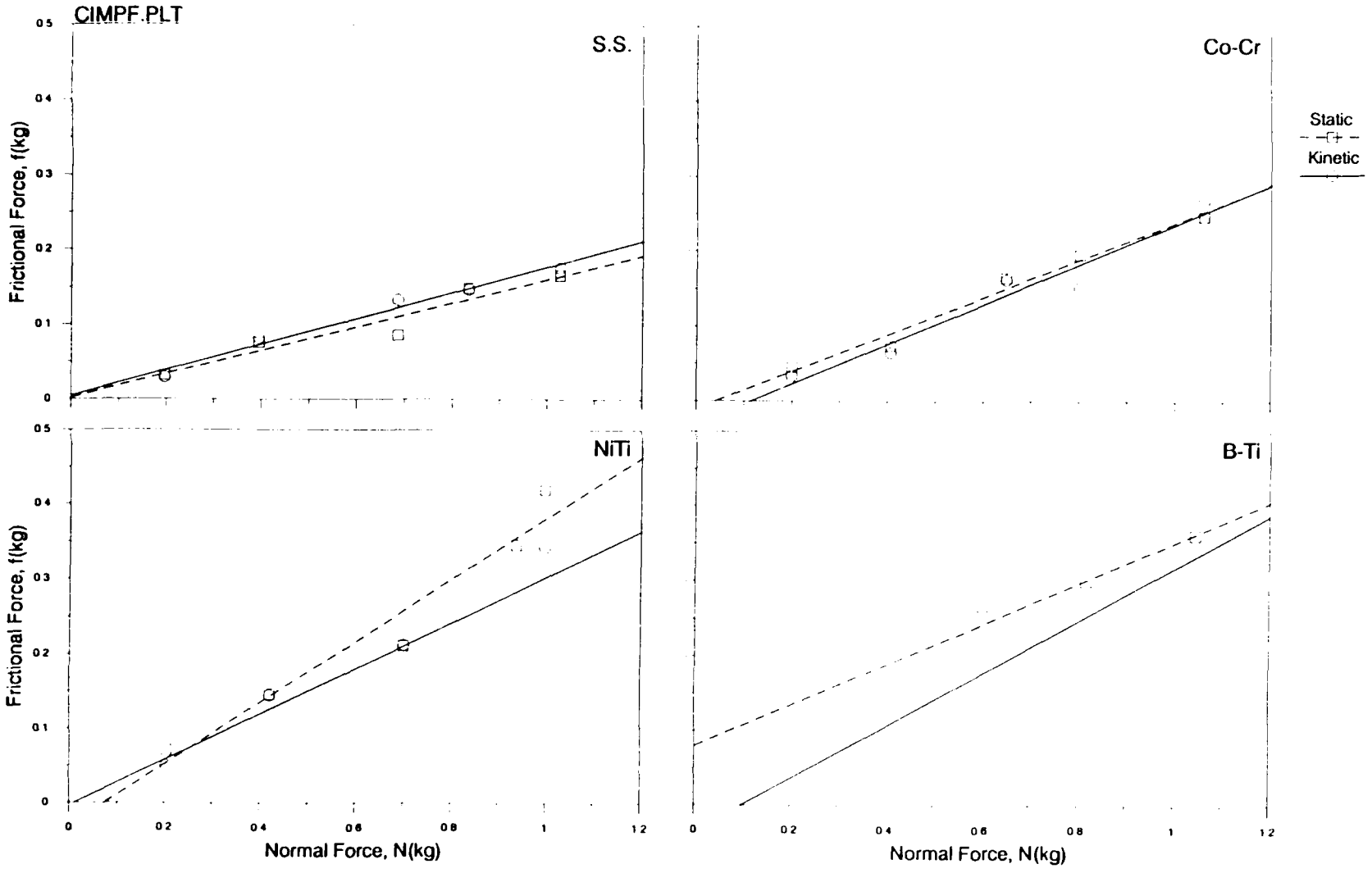

Figure 22. Plots of the frictional force (f=P/2) versus normal force (N) for C+ implanted stainless steel against four arch wire alloys. Based upon the static and kinetic data which is reported in Table 6.

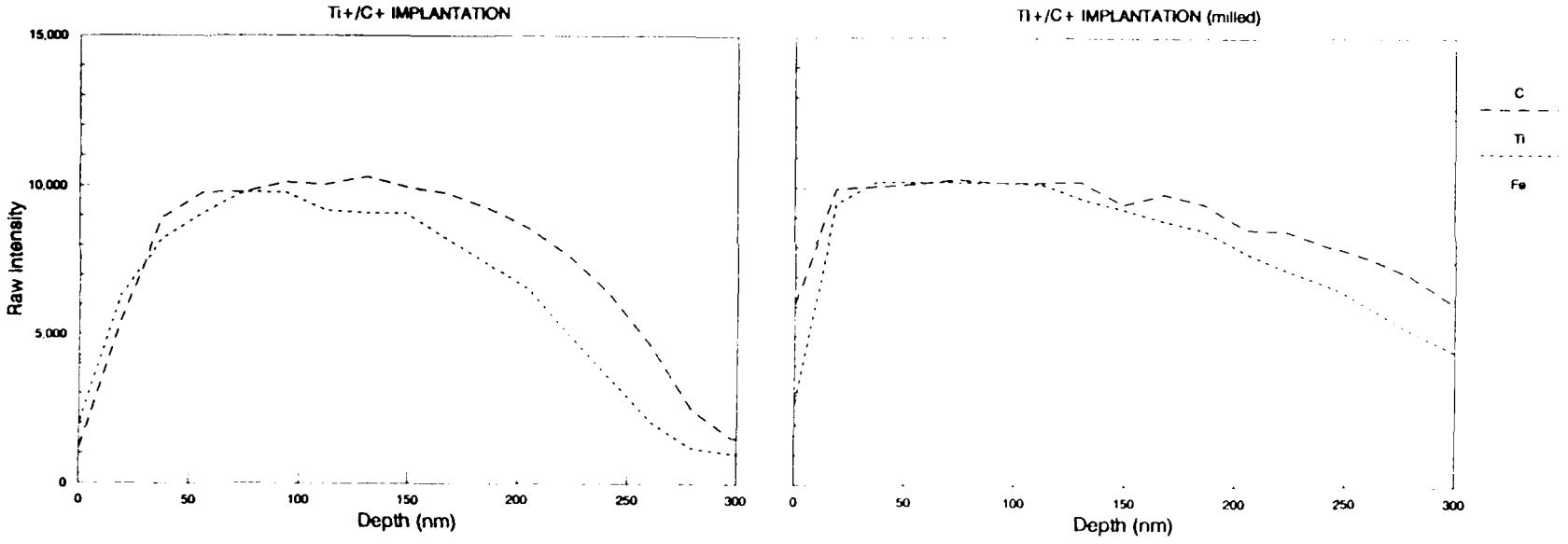

Figure 23. Auger electron spectroscopy comparison of the before and after milling for the Ti+/C+ implantation as reported in raw intensity.

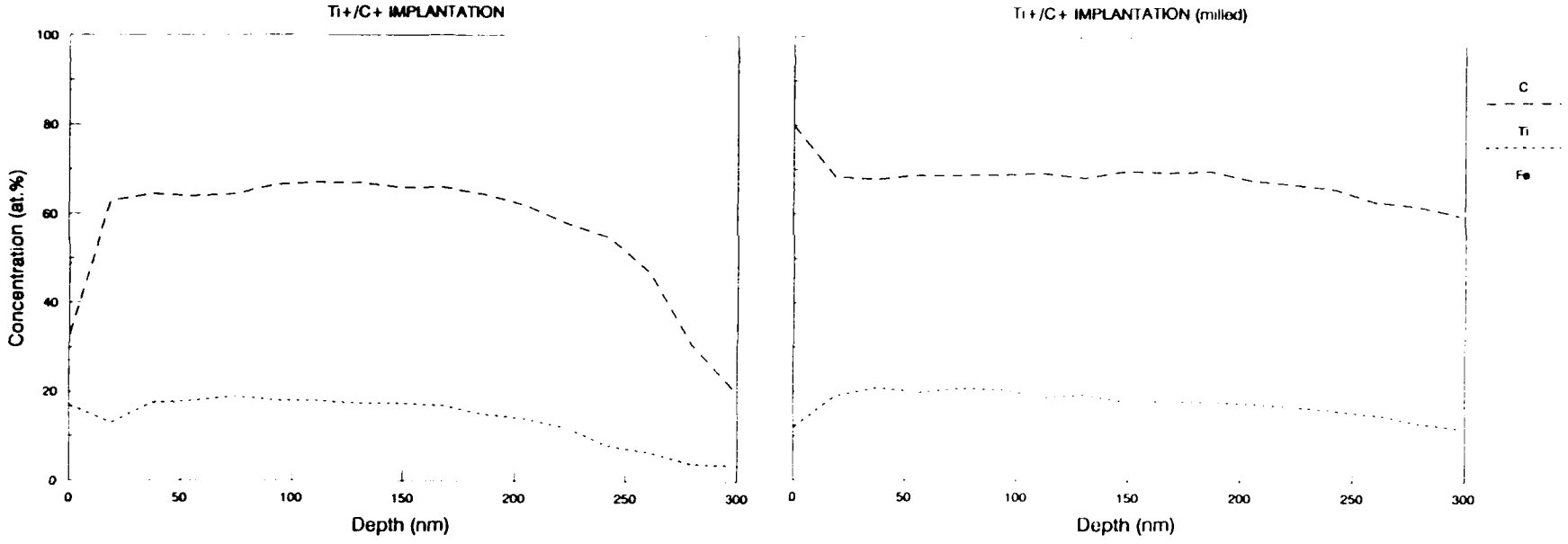

Figure 24. Auger electron spectroscopy comparison of the before and after milling for the Ti+/C+ implantation as reported in atomic percent concentration.

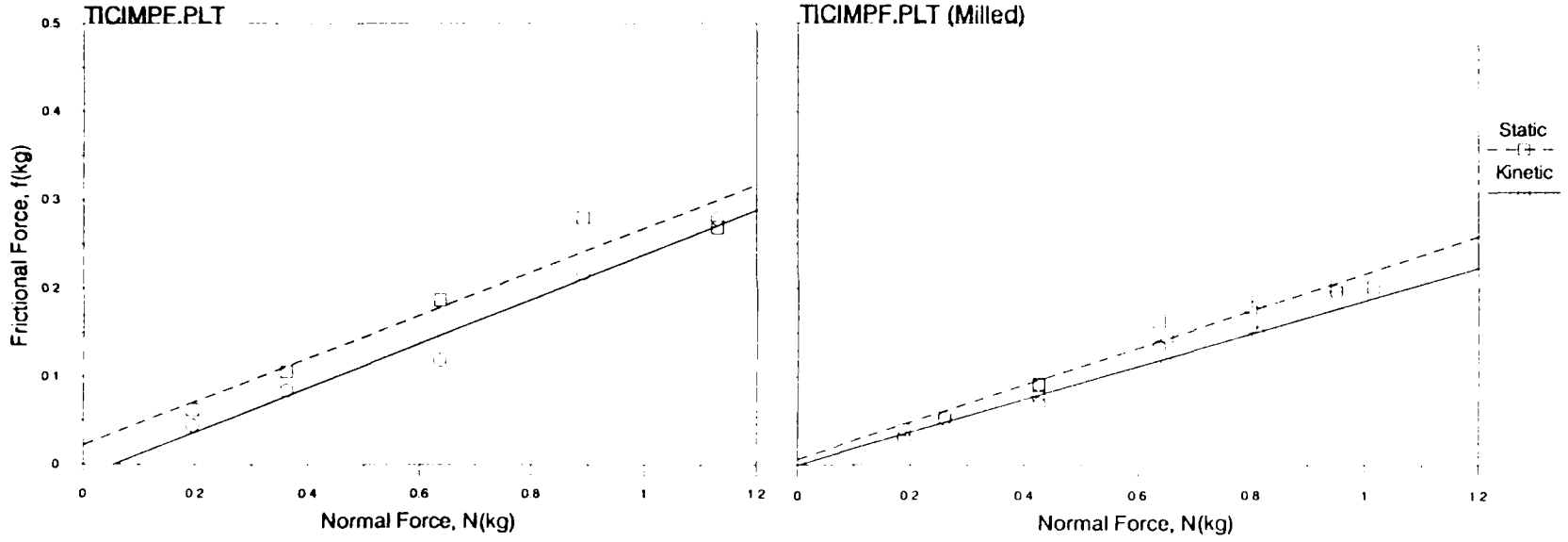

Figure 25. Plots of the frictional force (f=P/2) versus normal force (N) for Ti+/C+ implanted stainless steel against S.S. arch wires before and after milling. Based upon the static and kinetic regression data.

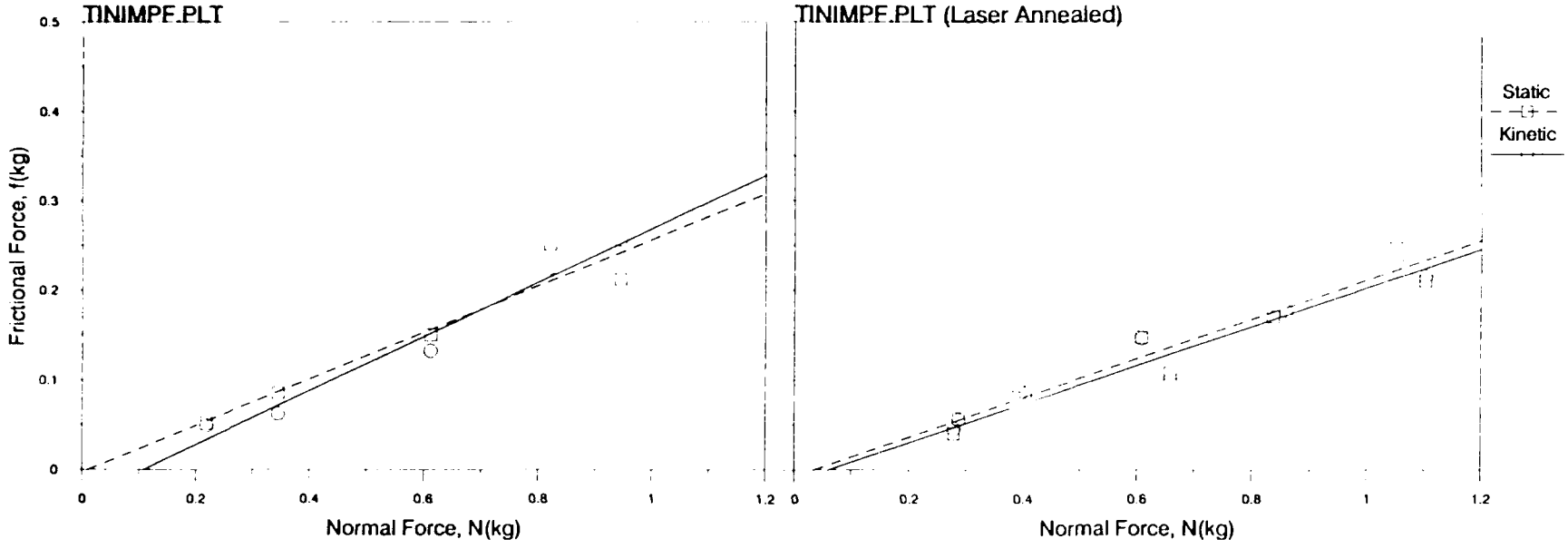

Figure 26. Plots of the frictional force (f=P/2) versus normal force (N) for Ti+/N+ implanted stainless steel against S.S. arch wires before and after laser annealing. Based upon the static and kinetic regression data.

ABSTRACT

STEPHEN W. ANDREWS. Surface Modification of Orthodontic Bracket Models via Ion Implantation: Effect on Coefficients of Friction. (under the direction of ROBERT P. KUSY, PH.D.)

In an effort to reduce the unwanted effects of friction, ion implantation of bracket models was accomplished and tested against the four major orthodontic alloy groups, [stainless steel (S.S.), cobalt-chromium (Co-Cr), nickel-titanium (NiTi), and beta-titanium (β-Ti)]. Stainless steel right-hand cylinders, 1/4" x 1/2", simulated orthodontic brackets. In addition to control samples, the polished faces of these cylinders were implanted with N+, Ti+/N+, N+/C+, N+/Cr+, Ti+, Ti+/C+, and C+. All were implanted at 2 x $10^{17}/cm^2$ except Ti+ (4 x $10^{17}/cm^2$) and Cr+ (3 x $10^{17}/cm^2$). Quality control was insured using Auger spectroscopy, specular reflectometry, and microhardness tests. Using an Instron tester the two cylinder flats were drawn along each arch wire at 1cm/min at 34°C in saliva. Frictional forces were measured, and both the coefficient of static friction, μ_s, and the coefficient of kinetic (sliding) friction, μ_k, were determined while varying the normal forces from 0.2 to 1kg.

The kinetic coefficients of the arch wires against the control S.S. models measured 0.163, 0.143, 0.240, and 0.312, respectively ($P \leq 0.01$). Results reveal that, with few exceptions, the S.S. control cylinders yielded lower μ_k's than the implanted cylinders. Any improvement seen with the implantations were marginal at best.

BIBLIOGRAPHY

Allai, W.W. 1984. A comparison of frictional forces during simulated canine retraction on a continuous edgewise archwire. Alumni Bull., I.U.S.D. Spring: 85.

American Society for Metals Handbook Committee. Metals Handbook, Vol. 8 Mechanical Testing, ed. 9, United States, 1985, American Society for Metals, 90-91.

Andreasen, G.F. and Quevedo, F.R. 1970. Evaluation of frictional forces in the 0.022 x 0.028 edgewise bracket in vitro. J. Biomech. 3: 151-160.

Bowden, F.P. and Tabor, D. Friction and lubrication, ed. 1, New York, 1956, John Wiley, 146.

Davis, L.E., MacDonald, N.C., Palmberg, P.W., Riach, G.E., and Weber, R.E. Handbook of Auger Electron Spectroscopy, ed. 2. Philadelphia, 1978, Physical Electronics Industries, Inc., p.1.

Dillich, S.A., Bolster, R.N., and Singer, I.L. 1984. Friction and wear behavior of a cobalt-based alloy implanted with Ti or N. Mat. Res. Soc. Symp. Proc. 27: 637-642.

Follstaedt, D.M. and Meyers, S.M., 1981. Ion beam modification of materials. Nucl. Instrum. Meth. 209/210: 1023-1031.

Follstaedt, D.M., Yost, F.G., and Pope, L.E. 1984. Microstructures of stainless steels exhibiting reduced friction and wear after implantation with Ti and C. Mat. Res. Soc. Symp. Proc. 27: 655-660.

Frank, C. A. and Nikolai, R. J. 1980. A comparative study of frictional resistances between orthodontic bracket and arch wire. Am. J. Orthod. 78: 593-609.

Gray, D.E. American Institute of Physics Handbook, ed. 3, New York, 1972, McGraw-Hill, 2-42 - 2-43.

Greenberg, A.R. and Kusy, R.P. 1979. A survey of specialty coatings for orthodontic wires. J. Dent. Res. 58: (Special Issue A) 98.

Hutchings, R., Oliver, W.C., and Pethica, J.B. Surface Engineering, ed. 1, New York, 1984, Saunders, Inc., 170-184.

Iwaki, M. 1987. Tribological properties of ion-implanted steels. Mat. Sci. and Eng. 90: 263-271.

Kapila, S., Angolkar, P., Duncanson, M.G.Jr., and Nanda, R.S. 1989. Effect of wire size and alloy on bracket-wire friction. J. Dent Res. 68: (Special Issue) 386.

Konishi, R.N., Whitley, J.Q., and Kusy, R.P. 1985. Surface roughness of a dental amalgam via a laser scattering test. Dent. Mater. 1: 55-57.

Kusy, R.P. and Whitley, J.Q. 1988a. Effects of surface roughness on the coefficients of friction in a model orthodontic system. In press.

Kusy, R.P. and Whitley, J.Q. 1988b. Effects of sliding velocity on the coefficients of friction in a model orthodontic system. In press.

Kusy, R.P., Whitley, J.Q., Mayhew, M.J., and Buckthal, J.E. 1988. Surface roughness of orthodontic archwires via laser spectroscopy. Angle Orthod. 58: 33-45.

Kusy, R.P. and Whitley, J.Q. 1989. Coefficients of friction of arch wires on stainless steel and polycrystalline alumina brackets: I. The dry state. In press.

McHargue, C.J. 1986. Ion implantation in metals and ceramics. Int. Met. Rev. 31: 49-76.

Nicolls, J. 1967-1968. Frictional forces in fixed orthodontic appliances. Dent. Prac. Dent. Rec. 18: 362-366.

Nikolai, R.J. Bioengineering Analysis of Orthodontic Mechanics. ed. 1, Philadelphia, 1985, Lea and Febiger, 53-56.

Nordling, C. and Oosterman, J. Physics Handbook, ed. 2, London, 1982, Chartwell-Bratt Ltd., 43.

Oliver, W.C., Hutchings, R., Pethica, J.B., Paradis, E.L., and Shuskis, A.J. 1984. Ion implanted Ti-6Al-4V. Mat. Res. Soc. Symp. 27: 705-710.

Oliver, W.C. 1989. Personal communication.

Pethica, J.B., Hutchings, R., and Oliver, W.C. 1983. Composition and hardness profiles in ion implanted metals. Nucl. Insrum. Meth. 209/210: 995-1000.

Pope, L.E., Yost, F.G., Follstaedt, D.M., Picraux, S.T., and Knapp, J.A. 1984. Friction and wear reduction of 440C stainless steel by ion implantation. Mat. Res. Soc. Symp. Proc. 27: 661-666.

Proffit, W.R. Contemporary Orthodontics. ed. 1, St. Louis, 1986, C.V. Mosby, 236.

Singer, I.L. and Jeffries, R.A. 1984a. Processing steels for tribological applications by titanium implantation. Mat. Res. Soc. Symp. Proc. 27: 637-642.

Singer, I.L. and Jeffries, R.A. 1984b. Friction, wear, and deformation of soft steels implanted with Ti and N. Mat. Res. Soc. Symp. Proc. 27: 667-672.

Sioshansi, P. 1987. Surface modification of industrial components by ion implantation. Mat. Sci. Engineering 90: 373-377.

Sioshansi, P., and Au, J.J. 1985. Improvements in sliding wear for bearing-grade steel implanted with titanium and carbon. Mat. Sci. Eng. 69: 161-166.

Sioshansi, P., Oliver, R.W., and Matthews, F.D. 1985. Wear improvement of surgical titanium alloys by ion implantation. J. Vac. Sci. Technol. A: 3.

Stannard, J.G., Gau, J.M., and Hanna, M.A. 1986. Comparative friction of orthodontic wires under dry and wet conditions. Am. J. Orthod. 89: 485-491.

AUTHOR: STEPHEN W. ANDREWS

TITLE: Surface Modification of Orthodontic Bracket Models via Ion Implantation: Effect on Coefficients of Friction.

RANK: Major

BRANCH: U.S. Air Force, Dental Corps

DATE: 1989

Pages: 82 (including introductory pages)

DEGREE: M.S.

SCHOOL: Department of Orthodontics
School of Dentistry
University of North Carolina